

Deanship of Graduate Studies  
Al-Quds University

Study of Environmental Radioactivity in Jerusalem and  
Bethlehem by in-situ Gamma Ray Spectroscopy

By

Hussein Yousef Hussein Al-Masri

M.Sc. Thesis

Jerusalem-Palestine

1427/2006

Study of Environmental Radioactivity in Jerusalem and  
Bethlehem by in-situ Gamma Ray Spectroscopy

Prepared By:

Hussein Yousef Hussein Al-Masri

B.Sc. Medical Imaging, College of Health Professions-  
Palestine

Supervisor: Dr. Adnan Lahham

A thesis Submitted in Partial Fulfillment of Requirements of  
the degree of Master of Science in  
Environmental Studies

Department of Earth and Environmental Sciences

Faculty of Science and Technology- Al-Quds University

1427/20

Al-Quds University  
Deanship of Graduate Studies  
Environmental Studies  
Department of Earth and Environmental Sciences

### Thesis Approval

Study of Environmental Radioactivity in Jerusalem and Bethlehem by in-situ  
Gamma Ray Spectroscopy




Prepared By: Hussein Y. H. Al-Masri

Registration No. 20312220

Supervisor: Dr. Adnan Lahham

Master thesis submitted and accepted: 21/ 6 / 2006

The names and signatures of examining Committee members are as follows:

1. Head of Committee: Dr. Adnan Lahham      Signature.....
2. Internal Examiner: Dr. Amin Leghrouz      Signature.....
3. External Examiner: Dr. Adnan Joudeh      Signature.....

Jerusalem- Palestine

1427/2006

# **Dedication**

To

My Beloved Parents, Family, Teachers and Friends



**Declaration:**

I Certify that this thesis submitted for the degree of Master is the result of my own research, except where otherwise acknowledged, and that this thesis (or any part of it) has not been submitted for a higher degree to any other university or institution.

Signed.....

Hussein Yousef Hussein Al-Masri

Date: 24/6 / 2006

## **Acknowledgements**

First of all, Great thanks to the Almighty Allah, the Creator of the Universe. Great thanks are extended to my supervisor and advisor Dr. Adnan Lahham for his continuous and generous advising and guidance through the whole research. Furthermore, much appreciation is given to my teacher Mr. Mustafa Awiess for his continuous encouragements to continue my higher study and to my colleagues at the Department of Earth and Environmental Sciences in Al-Quds University, especially Mr. Mohammed Sbaih for his great help and cooperation in making the measurements' location map.

## Abstract

This study deals with the qualitative and quantitative evaluation of environmental radioactivity in the areas of Jerusalem and Bethlehem. For this purpose, the technology of in-situ gamma ray spectroscopy is used. The detection system consist of a 3" × 3" inch NaI(Tl) detector connected to multichannel analyzer InSpector 2000 from Canberra instruments and laptop computer.

Gamma ray spectra were collected with the detector placed 1 meter above the ground surface. Measurements are performed outdoor in open terrain and also indoor at 15 locations. Energy and efficiency calibrations are achieved experimentally using standard gamma emitting radioactive sources of known activities and also theoretically using Monte Carlo calculations. The majority of identified radionuclides are naturally occurring gamma emitting sources (the decay products of  $^{238}\text{U}$ ,  $^{232}\text{Th}$  and  $^{40}\text{K}$ ). The only identified anthropogenic radionuclide is  $^{137}\text{Cs}$ . This radionuclide is found in two locations; in the town of Beit Sahour and in the Doha town near Bethlehem. The most probable origin of  $^{137}\text{Cs}$  is the Chernobyl accident occurred in the former USSR in 1986.

The effect of rain is also investigated and it is found that, rain affects mainly the low energy parts of the measured  $\gamma$ -ray spectra at energies corresponding to the decay progenies of  $^{238}\text{U}$ . The attenuation of photons emitted from soil in these parts of the spectra is due to the retention of Radon gas in soil pores filled with water, which prevents Radon and its decay progeny from escaping from soil and reach the detector.



The ratio of outdoor to indoor radionuclide concentrations is also determined and found to be in good agreement with the ratio of outdoor to indoor  $\gamma$ -dose rate from terrestrial radiation.

The average activities of  $^{40}\text{K}$ ,  $^{214}\text{Bi}$ ,  $^{208}\text{Tl}$  were determined and they are  $(177 \pm 26 \text{ Bqkg}^{-1})$ ,  $(17 \pm 2.5 \text{ Bqkg}^{-1})$  and  $(14 \pm 2.1 \text{ Bqkg}^{-1})$  respectively. Derived average concentrations of U and Th are  $(2 \pm 0.3 \text{ ppm})$  and  $(4 \pm 0.6 \text{ ppm})$  respectively. The sensitivity of the detection system is evaluated by calculating the minimum detectable activity (MDA) of  $^{40}\text{K}$ , MDA is found to be around  $1 \text{ Bqkg}^{-1}$ .

## دراسة النشاط الاشعاعي البيئي في منطقتي القدس وبيت لحم باستخدام مطيافية أشعة جاما الحقلية

### ملخص

تقدم هذه الدراسة تقديرا نوعيا وكميا للنشاط الاشعاعي البيئي في منطقتي القدس وبيت لحم. ولتحقيق ذلك استعملت تقنية مطيافية أشع جاما الحقلية. يتكون نظام القياس من مكشاف اشعاع وميض (بلورة يوديد الصوديوم المطعم بعنصر الثاليوم) بحجم "3"×"3" انش متصل مع محلل طيف من نوع Inspect 2000 من شركة كانبيرا وكذلك مع جهاز كمبيوتر محمول. اما عملية قياس أطياف أشعة جاما فقد تمت بوضع المكشاف على ارتفاع متر واحد فوق سطح الارض. وقد أجريت القياسات في الحقل وكذلك في داخل البيوت في خمسة عشر موقعا. وتمت معايرة نظام القياس بطريقه تجريبية باستخدام مصادر لأشعة جاما ذات اشعاعية معروفة وكذلك بالطرق النظرية باستخدام النمذجة بواسطة طريقة Monte Carlo. ان اغلب العناصر المشعة التي تم التعرف عليها في التربة هي من العناصر المشعة الطبيعية التي تصدر اشعة جاما (نواتج انحلال اليورانيوم والثوريوم وكذلك نظير البوتاسيوم المشع  $^{40}\text{K}$ ) وقد تم اكتشاف مصدر مشع اصطناعي وحيد وهو عنصر السيزيوم  $^{137}\text{Cs}$  وذلك في موقعين في بلدة بيت ساحور وفي بلدة الدوحة بالقرب من بيت لحم. وأغلب التوقعات أن مصدر هذا العنصر هو حادثة مفاعل تشيرنوبيل التي حدثت في الاتحاد السوفيتي السابق عام 1986.

وتتمت أيضا دراسة أثر الامطار في توهين أطيف اشعة جاما المنبعثة من التربة. وقد تبين ان الامطار تؤثر خاصة على الأجزاء من الطيف ذي الطاقات المنخفضة وبالذات الاجزاء من طيف أشعة جاما التي تعود لنواتج انحلال عنصر اليورانيوم  $^{238}\text{U}$ . ويظهر أن توهين الفوتونات في تلك الأجزاء

من الطيف سببه انحباس غاز الرادون في التربة المشبعة بالماء بحيث يمنع هذا الماء انفلات غاز الرادون من التربة وبالتالي وصوله الى منطقة مكشاف الإشعاع. كذلك تم حساب معدل قراءات المكشاف داخل البيوت وخارجها ووجد أن هذا المعدل يتوافق مع نسبة معدل الجرعة الجامي خارج البيوت وداخلها.

لقد تم حساب إشعاعية كل من العناصر التالية  $^{40}\text{K}$ ،  $^{214}\text{Bi}$  و  $^{208}\text{Tl}$  وكانت النتائج كالتالي:  
( $177 \pm 26$  بكريل/كلغم) ، ( $17 \pm 2.5$  بكريل/كلغم) و ( $14 \pm 2.1$  بكريل/كلغم) على التوالي. وكذلك اشتقت تراكيز اليورانيوم والثوريوم وكانت ( $2 \pm 0.3$  جزء من مليون) لليورانيوم و ( $4 \pm 0.6$  جزء من مليون) للثوريوم. أما حساسية نظام القياس فقد تم تحديدها عن طريق حساب النشاط الإشعاعي الأدنى الذي يمكن قياسه لنظير البوتاسيوم المشع  $^{40}\text{K}$  وكانت القيمة 1 بكريل/كلغم.

---

## Table of Contents

---

	Page
<b>Declaration</b>	<b>i</b>
<b>Acknowledgements</b>	<b>ii</b>
<b>English Abstract</b>	<b>iii</b>
<b>Arabic Abstract</b>	<b>v</b>
<b>Table of Contents</b>	<b>vii</b>
<b>List of Tables</b>	<b>x</b>
<b>List of Figures</b>	<b>xi</b>
<b>Definitions and Abbreviations</b>	<b>xiv</b>
<b>Chapter I: Radioactivity in the Environment of Man</b>	<b>1</b>
<b>1.1 Introduction</b>	<b>1</b>
<b>1.2 Types of Environmental Radioactivity</b>	<b>2</b>
<b>1.2.1 Sources of Natural Radiation Exposures</b>	<b>3</b>
<b>a. Cosmic Radiation</b>	<b>3</b>
<b>b. Cosmogenic Radionclides</b>	<b>4</b>
<b>c. Primordial Radionuclides</b>	<b>6</b>
<b>d. Anthropogenic Radionuclides</b>	<b>9</b>

1.3 Decay Series of Natural Radionuclides and <sup>40</sup> K	11
1.4 Natural Radioactivity in Soil	15
1.5 The Motivation for this Study	15
1.6 Aims and Goals of the Study	16
1.7 Thesis Outline	16
<b>Chapter II: Monitoring and Mapping of Environmental Radioactivity</b>	<b>17</b>
2.1 Methods of Environmental Radioactivity Monitoring	17
2.2 Gamma Dose Rate	17
2.3 Gamma Radiation Mapping	18
2.3.1 Airborne Gamma Ray Spectroscopy (AGRS)	18
2.3.2 Car-borne Gamma Ray Spectroscopy (CGRS)	19
2.3.3 Ground Gamma Ray Spectroscopy	21
2.4 Analysis of Soil Samples	21
<b>Chapter III: In-Situ Gamma Ray Spectroscopy</b>	<b>22</b>
3.1 Gamma-Ray Spectroscopy	22
3.2 Properties of Gamma Ray Spectra	23
3.3 Portable Gamma Ray Spectroscopy	25
3.4 Environmental Factors Affecting $\gamma$ -Ray Spectroscopy	26
<b>Chapter IV: Methodology and Instrumentation</b>	<b>28</b>
4.1 Methods	28

<b>4.2 The NaI (TI) Gamma-ray Detection System</b>	<b>28</b>
<b>4.3 Electronics</b>	<b>29</b>
<b>4.3.1 Detector</b>	<b>29</b>
<b>4.3.2 Multi Channel Analyzer (MCA)</b>	<b>30</b>
<b>4.3.3 InSpector 2000 Portable Spectroscopy Workstation</b>	<b>30</b>
<b>4.3.4 Genie 2000 Basic Spectroscopy Software</b>	<b>31</b>
<b>4.4 Study Area</b>	<b>33</b>
<b>4.4.1 Abu Dies Geological Formation</b>	<b>37</b>
<b>4.4.2 Bethlehem Geological Formations</b>	<b>37</b>
<b>Chapter V: Results and Discussion</b>	<b>39</b>
<b>5.1 Calibration of the Spectrometer</b>	<b>39</b>
<b>5.1.1 Energy Calibration</b>	<b>39</b>
<b>5.1.2 Efficiency Calibration</b>	<b>40</b>
<b>5.2 Qualitative Analysis of Measured Gamma Ray Spectra</b>	<b>42</b>
<b>5.3 Indoor and Outdoor Measurements</b>	<b>45</b>
<b>5.4 Quantitative Analysis of Identified Radionuclides</b>	<b>48</b>
<b>5.5 Effect of Rain</b>	<b>54</b>
<b>5.6 Effect of Radon gas on indoor measurements</b>	<b>56</b>
<b>5.7 Sensitivity of Detection System</b>	<b>57</b>
<b>5.8 Conclusions and Recommendations</b>	<b>59</b>
<b>References</b>	<b>61</b>

---

**List of Tables**


---

	<b>Page</b>	
Table 1.1	Common cosmogenic radionuclides with their half-lives and activities	6
Table 1.2	Important primordial radionuclides and their half-lives	7
Table 1.3	Average activity mass concentrations and the dose rate in air 1 meter above the ground surface	8
Table 1.4	Examples of anthropogenic radionuclides with long half-lives	10
Table 1.5	Amount of naturally occurring radionuclides in typical soil of a volume 1 km × 1 km, and 1 m deep	15
Table 4.1	Measurement locations and area description	36
Table 5.1	Indoor to outdoor peak area ratios corresponding to $^{40}\text{K}$ , $^{214}\text{Bi}$ and $^{208}\text{Tl}$ at Al-Quds University and Doha City sites.	47
Table 5.2	Activity concentration of identified radionuclides	50
Table 5.3	$^{40}\text{K}$ , $^{238}\text{U}$ and $^{232}\text{Th}$ content in Palestinian soil	50
Table 5.4	Ratios of identified radionuclides concentrations	53
Table 5.5:	Attenuation ratios resulting form the effect of rain	56

---

## List of Figures

---

		<b>Page</b>
Figure 1.1	Average radiation exposure form natural and artificial sources	1
Figure 1.2	Possible pathways of radioactivity in the ecosystem of man	2
Figure 1.3	The decay series of $^{238}\text{U}$	12
Figure 1.4	The decay series of $^{232}\text{Th}$	12
Figure 1.5	Schematic energy level diagram of the radioactive decay of $^{40}\text{K}$	13
Figure 3.1	Basic gamma ray spectroscopy energy peaks	23
Figure 3.2	Gamma spectrum representing the escape peaks after pair production	24
Figure 3.3	Gamma ray spectra of Uranium, Thorium and Potassium	26
Figure 4.1	Schematic diagram illustrating the electronic setup of detection system used to acquire the data	29
Figure 4.2	In-situ gamma ray spectroscopy workstation	31
Figure 4.3	Measurement sites at Abu Dies (AQU)	34
Figure 4.4	Measurement sites at Bethlehem District along with geological formations	35
Figure 5.1	Gamma ray spectra of a point source radioactive standard of $^{137}\text{Cs}$ used for energy and efficiency calibration of the NaI(Tl) 3"× 3" detector	39
Figure 5.2	Gamma ray spectrum of a mixture of radioactive standards in Petri dish geometry used for energy calibration of the NaI(Tl) 3"× 3" detector	40
Figure 5.3	Counting efficiency of the used NaI(Tl) detector for various energies and activities of radionuclides homogeneously distributed in an area of 1 m <sup>2</sup> in soil at various depths using Monte Carlo simulation.	41



Figure 5.4	Counting efficiency as a function of energy for homogeneously distributed activity in the soil within a circle of 20 meters in radius and depth of 15 cm.	41
Figure 5.5	Low energy part of a measured $\gamma$ -ray spectrum showing the identified radionuclides of $^{214}\text{Pb}$ , $^{214}\text{Bi}$ and $^{137}\text{Cs}$ . This spectrum was collected in Beit Sahour near Bethlehem	42
Figure 5.6	High energy part of a measured $\gamma$ -ray spectrum collected in Beit Sahour showing the peaks which represent $^{40}\text{K}$ , $^{214}\text{Bi}$ and $^{208}\text{Tl}$ energy lines	43
Figure 5.7	Part of $\gamma$ -ray spectrum measured in Doha City indicating the presence of trace amounts of anthropogenic $^{137}\text{Cs}$	44
Figure 5.8	A Schematic Diagram of the Radioactive Decay of $^{137}\text{Cs}$	44
Figure 5.9	Differences in $\gamma$ -ray spectrum at low energies measured outdoor and indoor at Al-Quds University site.	45
Figure 5.10	Differences in $\gamma$ -ray spectrum at high energies measured outdoor and indoor at Al-Quds University site	46
Figure 5.11	Differences in $\gamma$ -ray spectrum at low energies measured outdoor and indoor at Doha City site	46
Figure 5.12	Background spectrum measured using upward detector geometry at 1 m height above the ground level at AQU.	49
Figure 5.13	Distribution of $^{40}\text{K}$ throughout measurement locations	51
Figure 5.14	Distribution of $^{214}\text{Bi}$ throughout measurement locations	51
Figure 5.15	Distribution of $^{208}\text{Tl}$ (the decay product of $^{232}\text{Th}$ ), throughout measurement locations	52

Figure 5.16	Relative distribution of eU and eTh throughout measurements sites	53
Figure 5.17	Ratios of eU / eTh throughout measurements sites	54
Figure 5.18	Low energy parts of $\gamma$ -ray spectra measured at the same location (College of Engineering) before and after rain representing $^{214}\text{Pb}$ and $^{214}\text{Bi}$ (decay products of $^{238}\text{U}$ ).	55
Figure 5.19:	High energy parts of $\gamma$ -ray spectra measured at the same location (College of Engineering) before and after rain representing $^{40}\text{K}$ , $^{214}\text{Bi}$ (decay product of $^{238}\text{U}$ ) and $^{208}\text{Tl}$ (decay product of $^{232}\text{Th}$ ).	55
Figure 5.20:	Comparison between $\gamma$ -ray spectra measured indoor at AQU in the first floor and in the basement.	57
Figure 5.21:	Method of minimum detectable activity (MDA) determination for $^{40}\text{K}$	58

## **Definitions and Abbreviations:**

**Absorbed Dose:** Absorbed dose is the amount of energy deposited in any material by ionizing radiation. It is a measure of energy absorbed per gram of material. The SI unit of absorbed dose is the gray. The special unit of absorbed dose is the RAD.

**ADC:** Analog to Digital Converter. A device which changes an analog signal to a digital signal.

**Alpha Particle:** A particle made up of two neutrons and two protons; it is identical to a helium nucleus and is the least penetrating of the three common types of radiation (the other two are beta particles and gamma rays), being stopped by a sheet of paper or a few centimeters of air. An alpha-emitting substance is generally not dangerous to a biological system, such as the human body, unless the substance has entered the system.

**Annihilation Radiation:** Radiation produced by the annihilation of a positron and an electron. For particles at rest, two photons with energy of 511 keV each are produced.

**AQU:** Al-Quds University.

**Background Radiation:** Radiation due to sources other than the sample, such as cosmic rays, radioactive materials in the vicinity of a detector or radioactive components of the detection system other than the sample.

**Background Subtraction:** The statistical process of subtracting the background level of radiation from a sample count.

**Backscattering:** The process of scattering or deflecting into the sensitive volume of a measuring instrument radiation that originally had no motion in that direction. The process is dependent on the nature of the mounting material, the shield surrounding the sample and the detector, the nature of the sample, the type of energy of the radiation, and the geometry.

**Becquerel:** The SI unit of activity, defined as one disintegration per second (dps).

**Beta Particle:** An elementary particle emitted from a nucleus during radioactive decay with a single electrical charge and a mass equal to 1/1837 that of a proton. A negatively charged beta particle is identical to an electron. A positively-charged beta particle is called a positron.

**Channel:** One of an MCA's memory locations for storage of a specific level of energy or division of time.

**Compton Scattering:** Elastic scattering of photons in materials, resulting in a loss of some of the photon's energy.

**Continuum:** A smooth distribution of energy deposited in a gamma detector caused by the partial absorption of energy from processes such as Compton scattering.

**Cosmic Rays:** Radiation, both particulate and electromagnetic, that originates outside the earth's atmosphere.

**Count:** A single detected event or the total number of events registered by a detection system.

**Curie:** The (approximate) rate of decay of 1 gram of radium; by definition equal to  $3.7 \times 10^{10}$  becquerels (or disintegrations per second). Also, a quantity of any nuclide having 1 curie of radioactivity.

**Daughter Nuclide:** A radionuclide produced by the decay of a parent nuclide and is sometimes called decay progeny.

**Dead Time:** The time that the instrument is busy processing an input signal and is not able to accept another input; often expressed as a percentage.

**Decay:** The disintegration of the nucleus of an unstable atom by spontaneous fission, by the spontaneous emission of an alpha particle or beta particle, isomeric transitions, or by electron capture.

**Detection Level:** The level of net signal that can be predicted to be detectable.

**Detector:** A device sensitive to radiation which produces a current or voltage pulse which may or may not correspond to the energy deposited by an individual photon or particle.

**Disintegration:** See decay.

**DPM:** Disintegrations per minute. One DPM equals 60 Becquerels.

**Dose:** The radiation delivered to the whole human body or to a specified area or organ of the body. This term is used frequently in whole body counting applications.

**Efficiency:** The fraction of decay events from a standard sample seen by a detector in the peak corresponding to the gamma ray energy of the emission, and stored by a detection system. Also called Peak Efficiency. Used to calibrate the system for quantitative analyses. Also used to specify germanium detectors, where the relative efficiency of the germanium detector is compared to a standard (3 x 3 in.) NaI(Tl) detector.

**Efficiency Calibration:** A function, a lookup table, or series of functions, which correlate the number of counts seen by the detection system in specific peaks with known activity corresponding to such emission energies in a radioactive sample.

**Electromagnetic Radiation:** A general term to describe an interacting electric and magnetic wave that propagates through vacuum at the speed of light. It includes radio waves, infrared light, visible light, ultraviolet light, X rays and gamma rays.

**Electron Volt:** The amount of kinetic energy gained by an electron as it passes through a potential difference of 1 volt. It is equivalent to  $1.602 \times 10^{-19}$  joules. It is a unit of energy, or work, not of voltage.

**Energy Calibration:** A function which correlates each channel in the displayed spectrum with a specific unit of energy. Allows peaks to be identified by their location in the calibrated spectrum.

**Escape Peak:** A peak in a gamma ray spectrum resulting from the pair production process, the subsequent annihilation of the photons produced, and escape from the detector of the annihilation photons. If both annihilation photons escape, and the rest of the original gamma energy is fully absorbed, a double escape peak is produced at an energy equal to the original gamma ray energy minus 1.022 MeV. If only one of the photons escapes, a single escape peak is produced at an energy equal to the original gamma ray energy minus 511 keV.

**Full Energy Absorption:** The absorption and detection of all of the energy of an incident photon. May take place as a direct photoabsorption or as a result of multiple Compton scatterings of the incident photons within the resolving time of the detection system.

**Full Energy Peak:** The peak in an energy spectrum of X-ray or gamma-ray photons that occurs when the full energy of the incident photon is absorbed by the detector.

**FWHM (Full Width at Half Maximum):** The full width of a peak measured at one-half of its maximum amplitude with the continuum removed. Defines the resolution of a spectroscopy system.

**Gamma Ray:** A photon or high-energy quantum emitted from the nucleus of a radioactive atom. Gamma rays are the most penetrating of the three common types of radiation (the other two are alpha particles and beta particles) and are best stopped by dense materials such as lead.

**Gray:** The SI unit of absorbed dose, defined as one joule per kilogram of absorbing medium.

**Half-life:** The time in which one half of the atoms of a particular radioactive substance decay to another nuclear form. Half-lives vary from millionths of a second to billions of years.

**Histogram:** A representation of data by vertical bars, the heights of which indicate the frequency of energy or time events.

**In Situ Counting:** Measurement and analysis of radioactivity performed at the sample's location.

**Integral:** The total sum of counts in the region of interest.

**Ionization:** The process by which an electrically neutral atom acquires a charge (either positive or negative).

**KeV (Kilo Electron Volt):** One thousand electron volts

**Limit of Detection:** The minimum amount of the characteristic property being measured that can be detected with reasonable certainty by the analytical procedure being used under specific measuring conditions. If the conditions change, the limit of detection will also change, even if the analytical procedure remains the same.

**Lower Limit of Detection (LLD):** The smallest net signal that can reliably be quantified. LLD is a measure of the performance of a system in terms of activity.

**MDA:** Minimum detectable activity. See lower limit of detection.

**MeV:** One million electron volts.

**Multi Channel Analyzer (MCA):** An instrument which collects, stores and analyzes time-correlated or energy-correlated events.

**Pair Production:** Creation of an electron- positron pair by gamma ray interaction in the field of a nucleus. For this process to be possible, the gamma ray's energy must exceed 1.022 MeV, twice the rest mass of an electron.

**Parent Nuclide:** A radionuclide that produces a daughter nuclide during decay.

**Peak:** A statistical distribution of digitized energy data for a single energy.

**Photoelectric Absorption:** The process in which a photon interacts with an absorber atom, the photon disappears completely, and the atom ejects a photoelectron (from one of its bound shells) in place of the photon.



**Photoelectron:** An electron released from an atom or molecule by means of energy supplied by radiation, especially light.

**Photomultiplier Tube (PMT):** A device for amplifying the flashes of light produced by a scintillator.

**Photon:** In quantum theory, light is propagated in discrete packets of energy called photons. The quantity of energy in each packet is called a quantum.

**Photopeak:** See Peak.

**Positron:** An elementary particle, an "anti-electron" with the mass of an electron but having a positive charge. It is emitted by some radionuclides and is also created in pair production by the interaction of high-energy gamma rays with matter.

**Progeny:** See daughter nuclide.

**Rad:** A special unit of absorbed dose. Equal to 0.01 gray.

**Radiation:** The emission or propagation of energy through matter or space by electromagnetic disturbances which display both wave-like and particle-like behavior. Though in this context the "particles" are known as photons, the term radiation has been extended to include streams of fast-moving particles. Nuclear radiation includes alpha particles, beta particles, gamma rays and free neutrons emitted from an atomic nucleus during decay.

**Radioactivity:** The emission of radiation from the spontaneous disintegration (decay) of an unstable nuclide.

**Radionuclide:** A radioactive isotope.

**Resolution:** The ability of a spectroscopy system to differentiate between two peaks that are close together in energy. Thus, the narrower the peak, the better the resolution capability. Measured as FWHM.

**Scattering:** A process that changes a particle's trajectory. Scattering is caused by particle collisions with atoms, nuclei and other particles or by interactions with electric or magnetic fields. If there is no change in the total kinetic energy of the system, the process is called elastic scattering. If the total kinetic energy changes due to a change in internal energy, the process is called inelastic scattering. See also backscattering.

**Scintillator:** A type of detector which produces a flash of light as the result of an ionizing event.

**Sievert:** The SI unit of dose equivalency (a quantity used in radiation protection). The sievert is the dose equivalent when the absorbed dose of ionizing radiation multiplied by the dimensionless factor Q (quality factor) and N (product of any other multiplying factors) stipulated by the International Commission on Radiological Protection is one joule per kilogram.

**Specific Activity:** The quantity of radioactivity per unit mass; for example, dpm/g or Bq/g.

**Spectrum:** A distribution of radiation intensity as a function of energy or time.

**Spectrometer:** A device used to count an emission of radiation of a specific energy or range of energies to the exclusion of all other energies. See also multichannel analyzer.

**Window:** A term describing the upper and lower limits of radiation energy accepted for counting by a spectrometer.

**X-Ray:** A penetrating form of electromagnetic radiation emitted during electron transitions in an atom to a lower energy state; usually when outer orbital electrons give up some energy to replace missing inner orbital electrons.

## Chapter I

### Radioactivity in the Environment

#### 1.1 Introduction

Radioactivity is a permanent part of our environment. The natural radiation sources that the humans are being exposed to include many components that can vary significantly with space and time (UNSCEAR, 1982). Human exposure to these sources comes from external exposure, and the inhalation and ingestion of naturally occurring radioactive materials of Uranium and Thorium and their decay products, as well as the Potassium  $^{40}\text{K}$  radioisotope.

Natural radiation and environmental radioactivity provide the major source of human exposure which comes from natural and artificial sources shown in Figure 1.1. Exposure to natural radiation is not uniform throughout the world and can vary substantially from place to place.

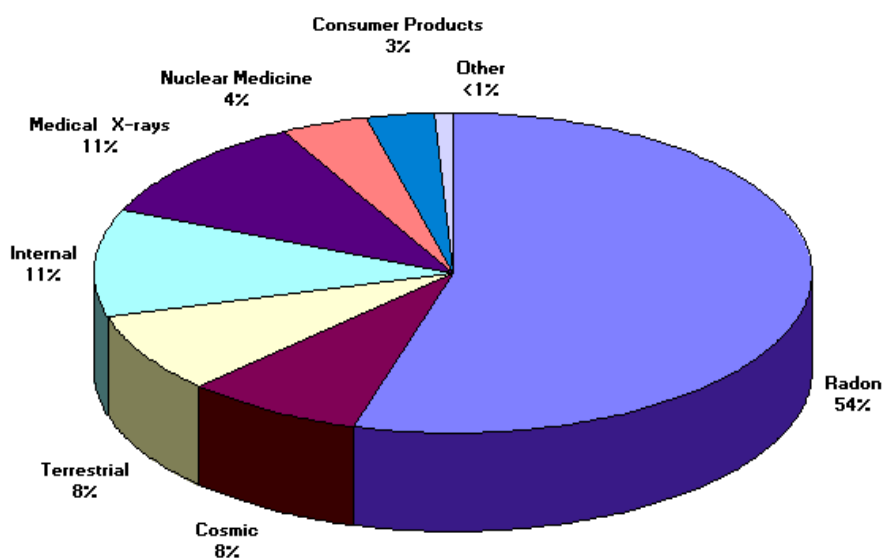


Figure 1.1: Average Radiation Exposure from Natural and Artificial Sources to the US Population (Taylor, 1996).

The two main components of natural exposure come from sources of extraterrestrial radiation (cosmic radiation) and radionuclides present in the earth crust and atmosphere (terrestrial radiation).

The difference between human-made sources of radiation and naturally occurring sources is the place from which the radiation originates. Social and industrial activities of the human beings has always changed this natural exposure and introduced new sources of radiation into the environment largely via the redistribution of natural activity (e.g. mining and minerals processing activities) or through the creation of man made radiation (e.g. medical X-rays, nuclear power and weapons testing) (Guy, 1988). Figure 1.2 shows possible pathways and contribution of natural sources of radiation to Man.

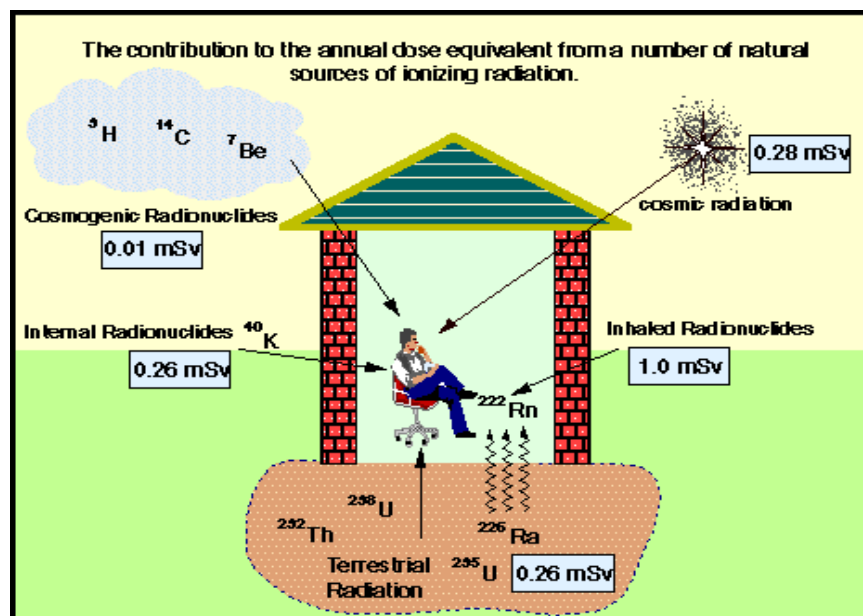


Figure 1.2: Possible pathways of radioactivity in the Ecosystem of Man (Giffin, 1996).

## 1.2 Types of Environmental Radioactivity

Radioactivity can be divided into four different types (Eisenbud and Gesell, 1997), and they can be placed in four general categories:

1. Cosmic radiation

2. Cosmogenic - formed as a result of cosmic ray interactions
3. Primordial - from before the creation of the Earth
4. Man made - produced by human activities (minor amounts compared to natural).

### **1.2.1 Sources of Natural Radiation Exposures:**

We are being continuously exposed to naturally occurring sources of radiation. Radiation from These sources is often referred to as background radiation. The two main sources of natural radiation exposures are:

- a) Sources of extraterrestrial origin of radiation (e.g. cosmic rays).
- b) Sources of terrestrial origin (e.g. radionuclides in the earth's crust, atmosphere, biosphere and hydrosphere).

The intensity of these sources of radiation can vary greatly in space and time; exposure to them occurs through the following mechanisms:

- External exposures to sources of ionizing radiation located outside the body, of which there are two sources, terrestrial and extraterrestrial.
- Internal exposures which comes from the inhalation and ingestion of radioactive materials into the body; these include radioisotopes of Carbon, Potassium, Uranium, Thorium and their decay products found on the earth. Many of the terrestrial radionuclides are naturally occurring and they have half-lives the same as the age of the earth ( $4.5 \times 10^9$  years).

#### **a. Cosmic Radiation:**

Cosmic radiation comes from the sun and outer space. It can be divided into two types, primary and secondary. Primary cosmic radiation is made up of extremely high energy particles (up to  $10^{18}$  eV), and are mostly protons, with some larger particles. A

large percentage of it comes from outside of our solar system and is found throughout space. Some of the primary cosmic radiation is from our Sun, produced during solar flares.

Little of the primary cosmic radiation penetrates to the Earth's surface; the vast majority of it interacts with the atmosphere. When it does interact, it produces the secondary cosmic radiation, or what we actually find here on Earth. These reactions produce other lower energy radiations in the form of photons, electrons, and neutrons that make it to the surface.

The atmosphere and the Earth's magnetic fields also act as shields against cosmic radiation, reducing the amount that reaches the Earth's surface. At sea level, the average annual cosmic radiation dose is about 26 mrem (University of California, 2000). At higher elevations, the amount of atmospheric shielding decreases and thus the dose increases. The total average annual dose to the general population from cosmic radiation is about 27 mrem.

#### **b. Cosmogenic Radionuclides:**

Cosmogenic radionuclides are produced mainly by activation, when high energy cosmic nucleons interact with atmospheric gases (e.g. Nitrogen, Oxygen and Argon) in the stratosphere, troposphere, lithosphere and biosphere. The major sources of their production are the interactions involving the atmosphere.

Other sources of cosmogenic radionuclides include materials of extraterrestrial origin such as asteroids, meteors and comets which contain significant concentrations of cosmogenic radionuclides (up to  $17 \text{ Bq.g}^{-1}$ ); (UNSCEAR, 1988); due to direct activation by cosmic rays over aeons of time. It is estimated that around 10000 metric tons of such material finds its way onto the Earth's surface each year. Assuming a constant rate of

inflow approximately  $10^{14}$  metric tons of such materials have been deposited since the earth was formed (UNSCEAR, 1988).

Additional sources include the atmospheric testing of thermonuclear devices which has significantly increased the concentrations of the above mentioned nuclides in the biosphere and human tissues. In addition, nuclear reactors also routinely release  $^{14}\text{C}$  and  $^3\text{H}$ . However, the total amounts are insignificant compared to the amounts generated naturally and by nuclear weapons testing.

Cosmogenic radionuclides appear to have relatively homogeneous distribution across the earth and have been detected in humans, topsoil, polar ice, surface rock, sediments, the biosphere, the sea floor and the atmosphere. The four cosmogenic radionuclides contributing to the majority of the dose to humans are  $^{14}\text{C}$ ,  $^3\text{H}$ ,  $^{22}\text{Na}$  and  $^7\text{Be}$ . Common cosmogenic radionuclides are listed in table 1.1. The first three of these are isotopes of major elements in the body; the first two contribute the majority of the dose from this source.  $^{14}\text{C}$  and  $^3\text{H}$  are formed when a fast neutron interacts with atmospheric Nitrogen as follows:



The predominant exposure pathways are by internal exposure due to inhalation and ingestion of food.



Table 1.1: Common cosmogenic radionuclides with their half-lives and activities.

Radionuclide	Symbol	Half-life	Source	Natural Activity
Carbon 14	$^{14}\text{C}$	5730 yr	Cosmic-ray interactions, $^{14}\text{N}(n,p)^{14}\text{C}$	(0.22 Bq/g) in organic material
Hydrogen 3 (Tritium)	$^3\text{H}$	12.3 yr	Cosmic-ray interactions with N and O, spallation from cosmic- rays, $^6\text{Li}(n, \alpha)^3\text{H}$	$(1.2 \times 10^{-3} \text{ Bq/kg})$
Beryllium 7	$^7\text{Be}$	53.28 days	Cosmic-ray interactions with N and O	(0.01 Bq/kg)

Some other cosmogenic radionuclides are  $^{10}\text{Be}$ ,  $^{26}\text{Al}$ ,  $^{36}\text{Cl}$ ,  $^{80}\text{Kr}$ ,  $^{14}\text{C}$ ,  $^{32}\text{Si}$ ,  $^{39}\text{Ar}$ ,  $^{22}\text{Na}$  and  $^{33}\text{P}$ . It should be noted that the direct activation of elements in the body can occur in persons directly exposed to cosmic rays, e.g. astronauts and passengers in supersonic aircraft flying at an altitudes of 10 Km or more. External exposures arising from cosmogenic radionuclides are insignificant compared to those from external exposures to primordial radionuclides.

### c. Primordial radionuclides:

The primordial radionuclides generate the majority of the collective dose to population arising from terrestrial background radiation. There are several dozen radionuclides present on earth with half lives of the order of the estimated age of the earth ( $\sim 4.5 \times 10^9$  years); these are assumed to represent what remains of primordial inventory set down billions of years ago. In terms of their contribution to human exposure, the following primordial radionuclides listed in table 1.2 are considered to be of primary importance.

Table 1.2: Important Primordial Radionuclides and their half-lives

Radionuclide	Half life ( Years)
$^{238}\text{U}$	$9.51 \times 10^9$
$^{232}\text{Th}$	$1.41 \times 10^{10}$
$^{40}\text{K}$	$1.28 \times 10^9$
$^{87}\text{Rb}$	$4.70 \times 10^{10}$
$^{235}\text{U}$	$6.96 \times 10^8$

Other primordial radionuclides include  $^{50}\text{V}$ ,  $^{123}\text{Te}$ ,  $^{115}\text{In}$ ,  $^{180}\text{W}$ ,  $^{113}\text{Cd}$ ,  $^{115}\text{In}$ ,  $^{138}\text{La}$ ,  $^{142}\text{Ce}$ ,  $^{147}\text{Sm}$ ,  $^{152}\text{Gd}$ ,  $^{209}\text{Bi}$  and others. The three radioactive decay series ( $^{238}\text{U}$ ,  $^{232}\text{Th}$  and  $^{235}\text{U}$ ) have several common characteristics; the parent radionuclide of each has a long half-life, each series has a gaseous isotope of Radon and each series ends with a stable isotope of Lead. On the other hand, Potassium is so widespread in the environment which contributes about one third of both the external terrestrial and internal dose from natural background radiation.  $^{40}\text{K}$  is a beta and gamma emitter, with an average concentration in rock of about 27000 ppm and in the ocean of about 380 ppm (Guy, 1988).

The radiation exposures arising from primordial radionuclides are commonly referred to as terrestrial radiation and comprise both external and internal exposures. External exposures arise from gamma rays produced by some of the primordial radionuclides. Internal exposures arise from the inhalation and ingestion of primordial radionuclides, which results in alpha, beta and gamma exposure of internal organs and tissues in the body.

Due to the ubiquitous presence of primordial radionuclides and their decay products in the environment (air, water, soil and foodstuffs) and in the humans, they contribute between 80-90% of the total natural background radiation dose to the human population. The external gamma dose rates above the ground arise from primordial radionuclides trapped in the soil.

The main sources are

$^{40}\text{K}$	35%
$^{238}\text{U}$ and its daughters	50%
$^{232}\text{Th}$ and its daughters	15%

The main contributors to the gamma dose rate are  $^{208}\text{Tl}$  and  $^{228}\text{Ac}$  from  $^{232}\text{Th}$  decay chain and  $^{214}\text{Pb}$  and  $^{214}\text{Bi}$  from  $^{238}\text{U}$  decay chain in the top 30 cm of soil (Guy, 1988). Typical average world readings in normal soils are listed in table 1.3, which gives these values for soil activity levels and the calculated dose rates at 1 meter in the air above the ground.

Table 1.3: Average Activity mass concentrations and the dose rate in air 1 meter above the ground surface (NCRP, 1994).

Radionuclide or Decay series	Dose rate per unit activity for wet mass concentration in soil ( $\text{nGy}\cdot\text{h}^{-1}$ per $\text{Bq}\cdot\text{Kg}^{-1}$ )	Average Activity from Mass Concentration in Wet Soil ( $\text{Bq}\cdot\text{Kg}^{-1}$ )	Dose rate at 1 m ( $\text{nGy}\cdot\text{h}^{-1}$ )
$^{238}\text{U}$	0.427	25 (10-50)	11 (4-20)
$^{232}\text{Th}$	0.662	25 (7-50)	17 (5-33)
$^{40}\text{K}$	0.043	370 (100-700)	16 (4-30)
Total	-	-	44

Note: The above values were calculated based on soil density of  $1.6 \text{ g}\cdot\text{cm}^{-3}$  and a water content of 10 % with the assumption of secular equilibrium in the decay chains (NCRP, 1994).

The average annual outdoor terrestrial dose rate in air from gamma radiation at 1 m above the ground is estimated to be  $44 \text{ nGy.h}^{-1}$  (UNSCEAR, 1982). There have been many surveys carried out in many countries to estimate the average exposure to gamma radiation. The country averaged outdoor dose rates ranged from 24 to  $85 \text{ nGy.h}^{-1}$  with a mean value of  $55 \text{ nGy.h}^{-1}$  (UNSCEAR, 1982).

Since most individuals spend a large fraction of their time inside the houses, it is important to measure the indoor dose rates. Many surveys have been done in some countries and these surveys indicate readings ranging from 23 to  $120 \text{ nGy.h}^{-1}$  with a mean value of  $70 \text{ nGy.h}^{-1}$  (UNSCEAR, 1982). The ratio of outdoor to indoor gamma dose rates varies between 0.8 to 2 with an average value of 1.3 (Guy, 1988). The elevated indoor dose rates rise mainly from materials used in the construction of those buildings.

#### **d. Anthropogenic Radionuclides :**

These are man-made radionuclides released into the environment through the testing of nuclear weapons and in the radioisotope manufacturing industry such as ( $^{137}\text{Cs}$ ,  $^{90}\text{Sr}$  and  $^{131}\text{I}$ ). A number of man's activities involve the use of radioactive materials. The most important of these is the use of radioactive materials for medical applications such as the diagnosis and treatment of cancer patients.

Some manufactured goods also contain small radioactive sources e.g. smoke detectors. Energy generation - for example nuclear energy production, extraction of oil and natural gas, and burning coal - also involves the release of small amounts of radioactivity to the environment. There is also a low level of residual radioactivity in the environment from the nuclear bomb tests of the 1950s and 1960s.

A severe nuclear accident, like Chernobyl, can add to this man-made radioactivity in the environment (Defra, 1999). Most anthropogenic radionuclides are short-lived, but some have half-lives of many years and are worthy of note, and are listed in table 1.4.

Table 1.4: Examples of anthropogenic radionuclides with long half-lives

Nuclide	Symbol	Half-life	Source
Tritium	$^3\text{H}$	12.3 yr	Produced from weapons testing and fission reactors; reprocessing facilities, nuclear weapons manufacturing
Iodine 131	$^{131}\text{I}$	8.04 days	Fission product produced from weapons testing and fission reactors, used in medical treatment of thyroid problems
Iodine 129	$^{129}\text{I}$	$1.57 \times 10^7$ yr	Fission product produced from weapons testing and fission reactors
Cesium 137	$^{137}\text{Cs}$	30.17 yr	Fission product produced from weapons testing and fission reactors
Strontium 90	$^{90}\text{Sr}$	28.78 yr	Fission product produced from weapons testing and fission reactors
Technetium 99	$^{99}\text{Tc}$	$2.11 \times 10^5$ yr	Decay product of $^{99}\text{Mo}$ , used in medical diagnosis
Plutonium 239	$^{239}\text{Pu}$	$2.41 \times 10^4$ yr	Produced by neutron bombardment of $^{238}\text{U}$ $(^{238}\text{U} + n \rightarrow ^{239}\text{U} \rightarrow ^{239}\text{Np} + \beta \rightarrow ^{239}\text{Pu} + \beta)$

Also, the global inventory of  $^{14}\text{C}$  and  $^3\text{H}$  has been increased from human activities, and it is sometimes necessary to measure these globally distributed radionuclides separately and to distinguish them from locally produced sources. The variability of man-

made sources of radiation and radioactivity is related directly to the population distribution and the level of technology found in different areas around the world. Deposition in an area depends upon wind and precipitation conditions (NCRP, 1994).

### 1.3 Decay Series of Natural Radionuclides and $^{40}\text{K}$

The decay series of  $^{238}\text{U}$  and  $^{232}\text{Th}$  shown in Figures 1.3 and 1.4; are characterized more or less by the initial part dominated by alpha decay and final part dominated by gamma-ray emission. This contributes to the difficulty in the radioactive measurements (Hendriks, 2001). During a series of radioactive decays, the original radioactive (parent) nucleus decays to another radioactive (daughter) nucleus until the end of the series, where a stable nucleus is formed ( $^{206}\text{Pb}$  in the case of  $^{238}\text{U}$  series and  $^{208}\text{Pb}$  for  $^{232}\text{Th}$ ) (Ivanovich and Harmon, 1982).

The number of daughter nuclei increases as a result of the decay of the parent nuclei and decreases as a result of the decay of its own, which leads after a long time to equilibrium which is reached when the production and the decay rates in the series are the same (Krane, 1988). Therefore, the activities of all the radionuclides in the chain must be equal and this phenomenon is referred to as secular equilibrium. This is usually a very accurate assumption except when daughter nuclei escape, for example when the radioactive gas  $^{222}\text{Rn}$  escapes in the decay series of  $^{238}\text{U}$ .

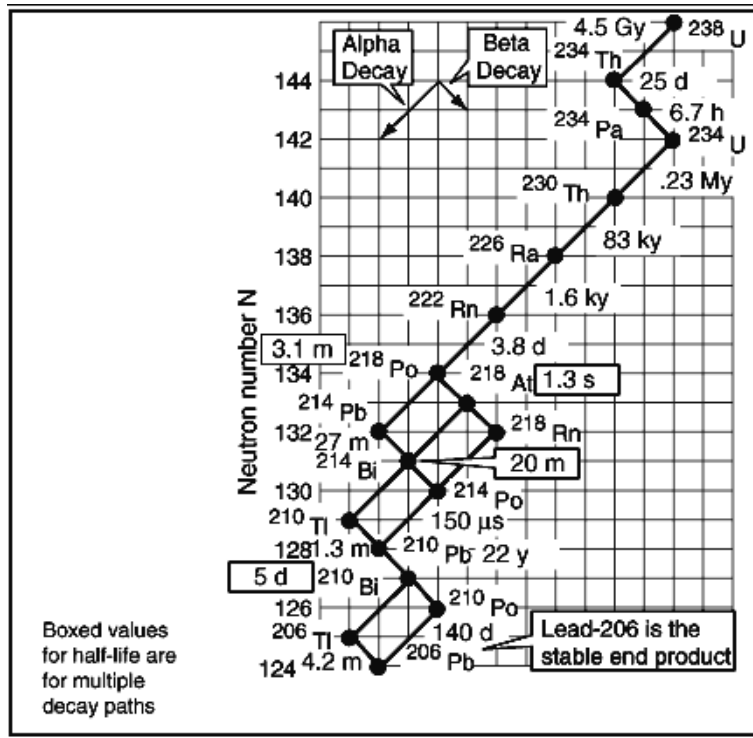


Figure 1.3: The decay series of  $^{238}\text{U}$

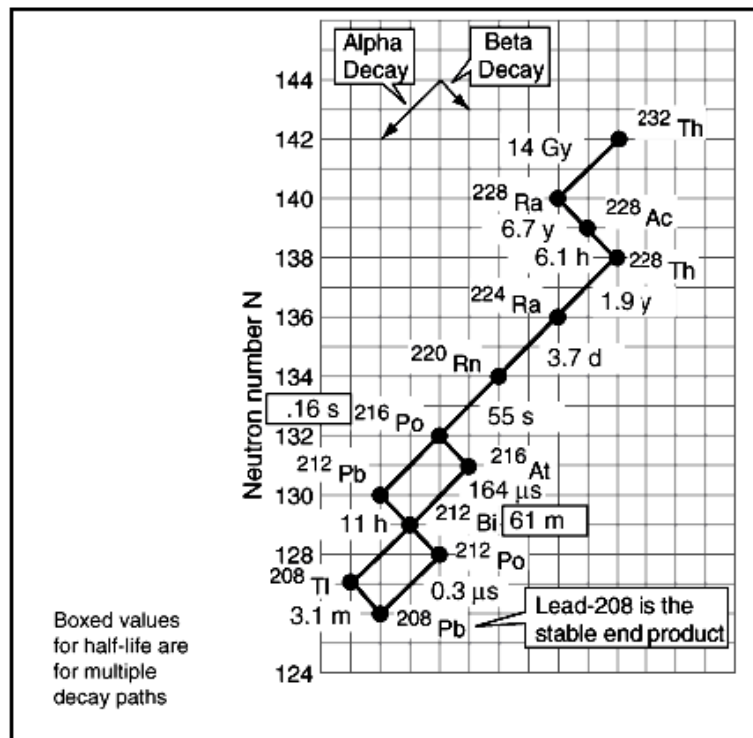


Figure 1.4: The decay series of  $^{232}\text{Th}$ .

The potassium element ( $^{40}\text{K}$ ), on the other hand is discussed here because it is a primordial radionuclide though it does not have decay series. It was discovered in 1807 and is the seventh most abundant and makes up about 2.4% by weight of the earth's crust. Ordinary Potassium is composed of three isotopes, one of which is  $^{40}\text{K}$  (0.0118%); a radioactive isotope with a half-life of  $1.28 \times 10^9$  years (BrainMass Inc., 2005), shown in Figure 1.5.

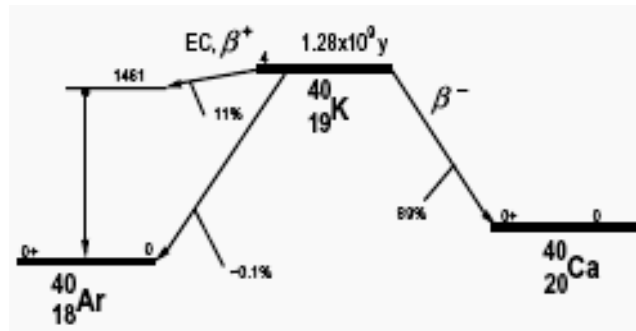


Figure 1.5: Schematic energy level diagram of the radioactive decay of  $^{40}\text{K}$  (Peterson, 1996).

Figure 1.5 shows two competing decay modes ( $\beta^-$ -decay and EC) to the stable  $^{40}\text{Ar}$ , while on the other hand there is 89% chance of decaying by  $\beta^-$  to  $^{40}\text{Ca}$ .

Most of the radioactivity associated with Uranium in nature is due to its progeny that are left behind in mining and milling. The gamma radiation detected by exploration geologists looking for uranium actually comes from associated elements such as Radium ( $^{226}\text{Ra}$ ) and Bismuth ( $^{214}\text{Bi}$ ), which over time have resulted from the radioactive decay of uranium. Uranium constitutes about 2 parts per million (ppm) of the Earth's crust (Eisenbud and Gesell, 1997).



In the decay series of, for example,  $^{238}\text{U}$ , the parent nucleus  $^{226}\text{Ra}$  decays to the daughter  $^{222}\text{Rn}$  by an  $\alpha$  decay, and  $^{222}\text{Rn}$  decays further to  $^{218}\text{Po}$  and consequently to  $^{214}\text{Pb}$ . Since  $^{222}\text{Rn}$  is a gas, it might escape the matrix and thus disturbing the secular equilibrium. In this event the activities of the  $^{222}\text{Rn}$  progeny will not be the same as their parents, and this is an indication of a disturbance of the secular equilibrium.

Therefore, to obtain secular equilibrium samples are generally sealed for the radon not to escape. This implies that the activity concentrations are the same for all members of the decay chain. When secular equilibrium is reached in the decay of  $^{238}\text{U}$  or  $^{232}\text{Th}$  it means that the activity concentrations of these nuclei can be determined by measuring activity concentration of their  $\gamma$ -emitting progeny. Therefore, the activity concentration of  $^{238}\text{U}$  and  $^{232}\text{Th}$  is reported in equivalent Uranium and equivalent Thorium as eU and eTh. The disturbance of secular equilibrium due to  $^{220}\text{Rn}$  (Thoron) is less significant due to its short half-life that is 55.6 seconds, implying that the Thoron build up will be negligible.

$^{232}\text{Th}$  is a naturally occurring, radioactive element which is found in small amounts in most rocks and soils, where it is about three times more abundant than uranium. Soil commonly contains an average of around 8 parts per million (ppm) of this nuclide (IAEA, 2003). The main pathways of exposure are ingestion and inhalation. It was found to be present in the highest concentrations in the pulmonary lymph nodes and lungs, indicating that the principal source of human exposure is inhalation of suspended soil particles (Eisenbud and Gesell, 1997).

## 1.4 Natural Radioactivity in Soil

Radionuclides are present in all rocks in varying amounts; table 1.5; and when released, they are easily mobilized in the environment. The high geochemical mobility of radionuclides in the environment allows them to move easily and to contaminate much of the environment with which humans come in contact.

Uranium, in particular, is easily mobilized in ground water and surface water. As a result, uranium and its decay product, radium, enter the food chain through irrigation waters, and enter the water supply through ground-water wells and surface-water streams and rivers. The health risks to humans are real, but the level of risk involved is not clearly defined because we do not yet know enough about the distribution and concentration of these radionuclides (Otton, 1994).

Table 1.5: Amount of naturally occurring radionuclides in typical soil of a volume  $1 \text{ km} \times 1 \text{ km}$ , and 1 m deep (Van Rooyen, 2002). Assuming soil density of  $1.6 \text{ g.cm}^{-3}$ .

Nuclide	Typical crustal activity concentration (Bq/kg)	Mass in $10^6 \text{ m}^3$ of radionuclide	Activity in $10^6 \text{ m}^3$
$^{238}\text{U}$	25	2800 kg	40 GBq
$^{232}\text{Th}$	40	15200 kg	65 GBq
$^{40}\text{K}$	400	2500 kg	630 GBq

## 1.5 The Motivation for this Study

This research is interested in the study of environmental radiation in Palestine in order to construct radiation maps for the whole country. The research began with measurements

in Bethlehem and Jerusalem Districts and in the future it will extend to cover all districts of our country.

## **1.6 Aims and Goals of the Study**

Study of environmental radioactivity has multiple goals:

1. To provide a reliable experimental database to estimate the human radiation exposure,
2. To record changes of environmental radioactivity and to establish a scientific basis on which human impact can be estimated with the goal to attain a sustainable development,
3. To understand the behavior of radionuclides in the environment and their pathways to Man,
4. To exploit the potential of radionuclides in the environment as natural and man-made tracers of environmental processes and, last but not least,
5. To give an evidence to the public about all facts of environmental radioactivity.

## **1.7 Thesis Outline**

The next chapter will discuss methods of monitoring the environmental radioactivity. Gamma ray spectroscopy used will be described in detail in chapter 3, while associated experimental work, instrumentation and methodology are discussed in chapter 4. The results and discussion will be presented and discussed in chapter 5 along with conclusions and recommendations.

## **Chapter II**

### **Monitoring and Mapping of Environmental Radioactivity**

#### **2.1 Methods of Environmental Radioactivity Monitoring**

Natural radioactivity comes from rocks and soils containing various proportions of radioactive elements. The disintegration of these elements produces a radiation (alpha, beta, and gamma) with specific energy levels. Gamma radiation is the best used for environmental radioactivity monitoring, because of its high penetrating power.

The most important ways to map gamma radiation are to measure gamma dose rate and to use different gamma ray spectroscopy methods such as airborne, car-borne and portable gamma ray spectroscopy which provide a method for measuring the concentrations of radioactive elements e.g. (U, Th, K) in rocks and soils.

#### **2.2 Gamma Dose Rate**

The dose rate basically is defined as the amount of energy deposited by radiation into a unit mass of irradiated matter per unit time. So, gamma or beta dose rate are used to describe any irradiation of matter by beta or gamma radiation. For the reason of gamma being more penetrating than beta, gamma dose rate is used for the description of terrestrial radiation and usually is expressed in nGy/h.

Gamma radiation from radionuclides deposited in the urban environment has contributed to air-dose rate and human external exposure. Compared to the dose rate in open fields, the

dose rate within a settlement has been always significantly lower because of photon absorption in building structures, especially those made of brick and concrete (Golikov et al., 2002).

The lower dose rates have been observed inside buildings, especially on the upper floors of multi-story buildings. Due to radioactive decay of the initial radionuclide mixture, wash-off from solid surfaces and soil migration, air-dose rates have been gradually decreasing with time. Another relevant parameter is the time dependence of the ratio of air-dose rate at an urban location compared to that in an open field (so-called location factor) due to radionuclide migration processes.

## **2.3 Gamma Radiation Mapping**

Airborne, car-borne or portable gamma ray spectroscopy is used for both regional and detailed mapping surveys for estimating the surface concentrations of the radionuclides. Also, gamma ray spectroscopy can be used to acquire information on lithology and mineralization in subsurface geological structures.

### **2.3.1 Airborne Gamma Ray Spectroscopy (AGRS):**

Airborne methods provide valuable, systematic coverage of large areas. The aim of airborne radiometric measurements is the determination of the radionuclide content of ground using the information of the direct terrestrial gamma radiation. All other contributions are annoying and have to be removed.

The development of the gamma-ray spectrometer in the early 1960's and its introduction into aircraft systems (requiring a significant increase in crystal volume) in the mid-60's marked a new era (NRC, 2004). In 1967 the first airborne gamma-ray surveys were done with

a helicopter. Such full-spectrum systems allowed the measurement of discrete 'windows' within the spectrum of gamma-ray energies to determine concentrations of individual radioelements (in particular, K, U, Th) and thus to begin mapping rocks by virtue of their characteristic radionuclide signatures (IAEA, 1991).

Airborne gamma-ray spectroscopy is an effective geological mapping tool in many different environments and has been applied to mineral, environmental, geothermal, hydrocarbon and even water investigations. The following are some of the most common applications for airborne gamma-ray spectroscopy surveys (Fugro, 2001):

- Mineral exploration: gold, mineral sands, uranium, rare earth elements;
- Geothermal exploration: potassic alteration;
- Hydrocarbon exploration: potassic/uranium alteration;
- Geological mapping: mineral, engineering and water exploration applications;
- Emergency response: fallout, nuclear contamination;
- Baseline surveys: for mining, nuclear reactor and industrial sites.

Gamma-ray measurements may also be applied in environmental monitoring such as mapping of radioactive contamination from fallout of nuclear accidents and plumes from power plants (e.g.  $^{137}\text{Cs}$  and  $^{60}\text{Co}$ ) (Grasty, 1998).

### **2.3.2 Car-borne Gamma Ray Spectroscopy (CGRS):**

Car-borne gamma ray spectroscopy has the advantage over portable systems because of much greater coverage for a given time and cost and over airborne systems because of its faster movement and improved resolution. These systems are more likely to be used for

environmental applications (e.g. mapping nuclear fallout, searching for lost radioactive sources) (IAEA, 2003). These systems are only to be used in areas where vehicles can reach, which is a not important matter for portable or airborne systems.

The operation is faster in car-borne systems in comparison to that of an airborne system. Hence, the resolution of the data is also much greater in car-borne systems than that of airborne ones.

However, the data taken from CGRS can have local variations due to the geological conditions, such as soil composition, soil moisture, surface water, and weathering. Also, topographic effects can have a significant effect on the information gained from car-borne systems, particularly where road cuts gives out new bedrock layers. Vegetation and buildings are other sources of noise. Radon gas may also produce some effects on the readouts (IAEA, 2003).

The efficiency of car-borne detection systems in identifying closely located sources depends largely on the detector geometry and on the materials used to construct the vehicles used for car-borne gamma ray spectroscopy (Grasty and Cox, 1997).

The advantages of using CGRS over AGRS are that the CGRS are more quickly done than AGRS. The second reason is that the CGRS can be operated all day long in comparison to AGRS. The third reason is that CGRS is the best for use in winter and snow conditions where the earth surface is covered by rain or snow, because of much easier removal of them when using CGRS. Also, in the case of nuclear fallout it is much easier and faster to change or replace a contaminated car or vehicle with a new or a clean one when emergency conditions occur (IAEA, 2003).

### **2.3.3 Ground Gamma Ray Spectroscopy:**

Ground gamma ray spectroscopy has been used since the 1960's for uranium exploration, geological mapping and environmental studies and are widely used for field studies. The following chapter is about portable gamma ray spectroscopy method, which is the type of spectroscopy used in this study.

### **2.4 Analysis of Soil Samples**

Monitoring concentrations of gamma-emitting radionuclides in surface soil provides insight to the transport, deposition, and accumulation of radioactive material in the environment as a result of historic atmospheric testing of nuclear weapons.

Therefore, radiation monitoring techniques include soil sampling and in-situ gamma spectroscopy. The in-situ gamma spectroscopy technique is preferred over soil sampling since it is a non-destructive analysis involving no sample collection or preparation. Therefore, no damage or alteration is done to the monitoring location and minimal waste generated.



## Chapter III

### In-Situ Gamma Ray Spectroscopy

#### 3.1 Gamma-Ray Spectroscopy

Gamma-Ray Spectroscopy (GRS) provides a direct measurement of the surface of the earth, with no significant depth of penetration. This at-surface characteristic allows us to reliably relate the measured radioactive element contrasts to mapped bedrock and surficial geology, and alteration associated with mineral deposits. All rocks, and the materials derived from them are radioactive, containing detectable amounts of a variety of radioactive elements. A gamma-ray spectrometer is designed to detect the gamma rays associated with these radioactive elements and to accurately sort the detected gamma rays by their respective energies. It is this sorting ability that distinguishes the spectrometer from instruments that measure only total radioactivity.

Many factors affect gamma spectroscopy such as the source intensity and the source-detector geometry. Other environmental factors such as rainfall, soil moisture, vegetation, and the distribution of airborne radioactive sources affect the measured gamma ray spectra (IAEA, 2003).

Measurement of gamma-emitting radionuclides in-situ has become feasible with the advent of scintillation detector (NaI (Tl)) and portable multi-channel analyzer (MCA). Data collected using the (NaI (Tl)) and digital MCA offers an opportunity to quickly set up the detection system in the field and still make accurate and reproducible measurements. Data are stored electronically until they can be downloaded to a personal computer for spectral analysis.

In-situ gamma ray spectroscopy is performed using a (NaI (Tl)) set on a tripod to fixed height of 1-m above the ground surface and using basic assumptions (e.g., soil density, radionuclide distribution). Assumptions used for in-situ gamma spectroscopy include a 1.3 g/cm<sup>3</sup> soil density, a field of view with a 10-m radius, and homogeneous radionuclide distribution in the top 30-cm of soil (IAEA, 2003).

### 3.2 Properties of Gamma Ray Spectra

Gamma rays interact with matter in three primary processes. These are photoelectric absorption, Compton scattering and pair production. Each one of these interactions is well represented in Figure 3.1.

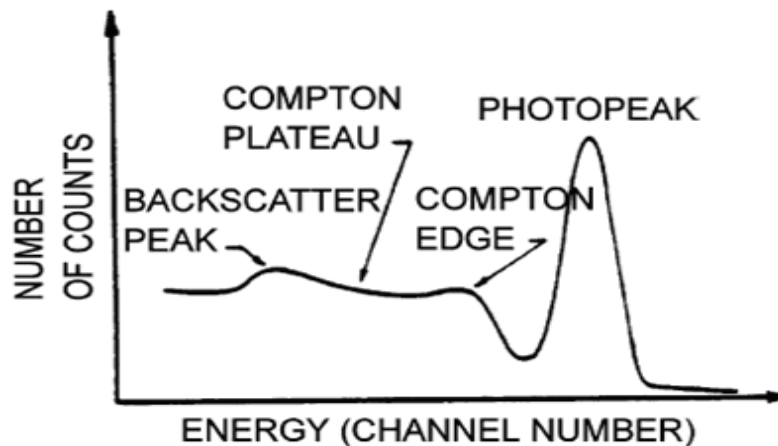


Figure 3.1: Basic Gamma ray spectroscopy energy peaks

Photoelectric absorption takes place when there is an interaction of a  $\gamma$ -ray photon with one of the bound electrons in an atom and all the energy of the photon is transferred to the electron. In Compton scattering, part of the  $\gamma$ -ray energy is transferred to the electron and the

photon is deflected or scattered. When the gamma ray is backscattered, only a proportion of its energy will be transferred to the electron, which gives rise to the Compton edge.

Pair Production is energetically possible if the  $\gamma$ -ray energy exceeds twice the rest mass of an electron that is 1.02 MeV. The entire energy is converted into an electron-positron pair. Annihilation then takes place in which the electron and positron rest masses are converted into two  $\gamma$ -rays, each with energy of 0.511 MeV, shown in Figure 3.2.

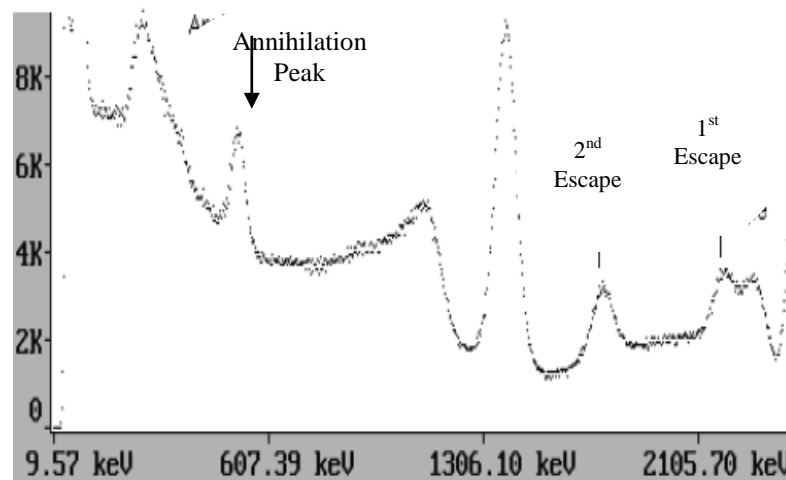


Figure 3.2: Gamma spectrum representing the escape peaks after pair production.

Each  $\gamma$ -emitting radionuclide gives a peak representing the energy of its corresponding photons. These photons are superimposed by Compton scattered photons which have a continuum of energies shown at the edge of the characteristic photons emitted by the isotope. This continuum is due to single and multiple scattering events between the source and the detector (Krane, 1988). Therefore, the shape of spectrum depends upon the source-detector geometry and on the detector response.

### **3.3 Portable Gamma Ray Spectroscopy**

The objective of portable gamma spectroscopy is to determine radioactivity of nuclides per unit area or unit volume of soil. Traditional methods generally give gross field surveys. However, field surveys with gross counting instrumentation do not identify specific radionuclides, and therefore cannot discriminate between natural radioactivity and man-made radioactivity (Canberra Inc., 2005).

Gross counting techniques also cannot detect small amounts of artificial radionuclides in the presence of larger amounts of other natural radionuclides. Any discrete sample taken for laboratory analysis will only identify what was at that specific, very small, sample site. This means that for cases where the contamination is not uniform, some hot spot areas could be missed. In-situ gamma spectroscopy, on the other hand, effectively detects all the radioactivity over as much as 100 m<sup>2</sup> of area, and for high energy gammas, even detects radioactivity buried below the surface of the soil. With in-situ gamma spectroscopy, there is a much higher probability that nothing will be missed. Then the samples must be prepared, analyzed, and the reports sent back to the user.

With in-situ gamma spectroscopy, the results are available immediately, with equivalent or better accuracy, and with less labor. With laboratory analyses, there is much labor involved, and a long turn around time for the analysis results. Samples must be collected and documented, labeled, and transported to a remote lab (with subsequent potential loss of chain-of-custody).

Each radionuclide of the three most common ones,  $^{40}\text{K}$  and the  $^{238}\text{U}$  and  $^{232}\text{Th}$  decay series has characteristic energy line spectra shown in Figure 3.3. These lines give the energy distribution of emitted photons from each source. Each line shows the energy and relative intensity of gamma ray emissions in the decay series.

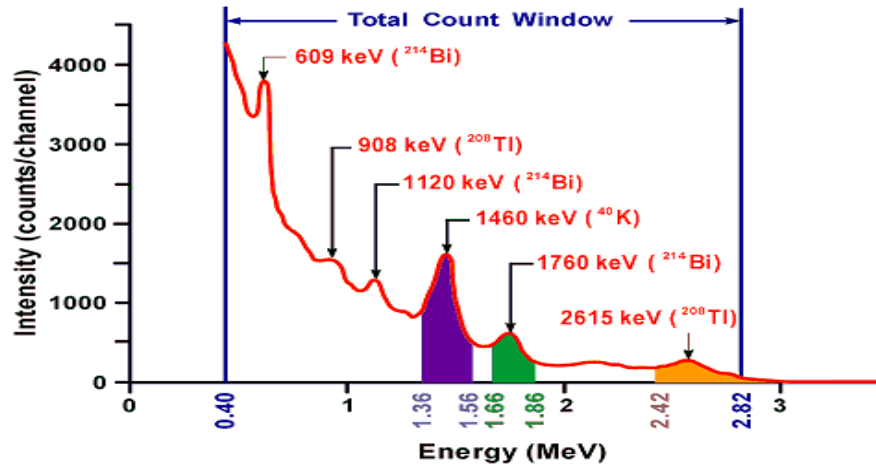


Figure 3.3: Gamma ray spectra of Uranium, Thorium and Potassium.

However, the energies shown in Figure 3.3 are reduced by Compton scattering which occur between the source and the detector. The relative contribution of scattered and unscattered photons to the gamma ray fluence rate thus depends on the source-detector geometry and on the amount of attenuating material between the source and the detector.

### 3.4 Environmental Factors Affecting $\gamma$ -Ray Spectroscopy

There are many factors that can affect the amount of measured gamma radiation. The variability of the naturally occurring radionuclides present in the soil due to geological formations is the largest contributor to variations in measurements. Meteorological conditions contribute to seasonal variability, as does cosmic variation (Bertoldo, 1998).

Other factors such as the materials between the detector and the source affect the intensity of measured radiation. In airborne gamma ray spectroscopy, the height of the detector above the ground has a large effect. This can affect the measured radiation by about 7%. Also, any cover above the ground can significantly reduce the radiation output from the earth's surface. For example, just 2 cm of cover can reduce by 35 percent the radiation penetrating to the ground surface. Dense vegetation and Snow cover can significantly attenuate radiation from the ground. Any changes in air density via increasing the air temperature or pressure may lead to an increase or decrease in the gamma radiation levels.

Close to the ground, atmospheric radon can affect the estimations of background radiation in airborne surveying. Soil moisture can be a significant source of error in gamma ray surveying. An increase in soil moisture will decrease the measured gamma dose rate.

Precipitation can have a large effect on Uranium estimation. Radon daughter products in air attach themselves to dust particles in the atmosphere. When precipitation occurs, these particles are washed out by rain onto the earth surface and can lead to observed increases of more than 2000 percent in Uranium ground concentrations (Charbonneau & Darnley, 1970). Gamma ray surveying should not be carried out during rainfall or shortly thereafter. It should be postponed at least for about three hours for the anomalous surface activity to decay away.

## Chapter IV

### Methodology and Instrumentation

#### 4.1 Methods

Most modern portable gamma ray spectrometers typically record either 256 or 512 channels of data in the energy range 0-3 MeV. Spectrum may shift to high energy parts due to power fluctuations. So, its stabilization is done by either a low-energy peak from a reference isotope (typically  $^{137}\text{Cs}$  at 0.662 MeV), or one of the natural radionuclide peaks (either  $^{40}\text{K}$  at 1.46 MeV or  $^{208}\text{Tl}$  at 2.62 MeV) (IAEA, 2003).

The instruments can record the full gamma ray spectrum as well as sum channels over broad energy windows for the in-situ estimation of  $^{40}\text{K}$ ,  $^{238}\text{U}$  and  $^{232}\text{Th}$  radioelement concentrations. The instruments' memory can store calibration constants as well as several thousands of field measurements and several hundreds of full energy spectra. Also, the use of large volume scintillation crystals and long time screening provide acceptable precision for quantitative analyses.

#### 4.2 The NaI (Tl) Gamma-Ray Detection System

The system is used to measure natural and anthropogenic activity concentrations in soil. It can also be used to measure artificial radioactivity such as the activities from cesium, strontium, etc. The available equipment in the field includes an NaI (Tl) detector, MCA, PC-based data acquisition system, Tripod stand and a  $^{137}\text{Cs}$  standard.

### 4.3 Electronics

The electronic system for the NaI (TI) scintillation detector is shown schematically in Fig. 4.1. The system consists of a Scintillation Detector (Model 802), preamplifier (Model 2007/2007P), amplifier (Canberra Model 2020), multi channel analyzer (InSpector 2000 DSP) and a laptop computer.

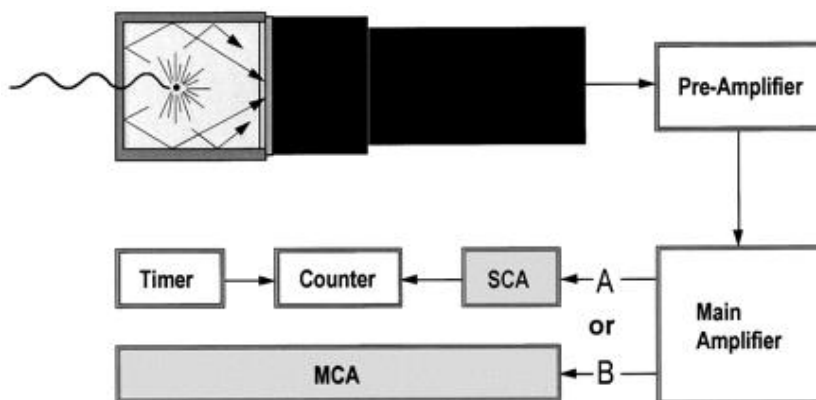


Figure 4.1: Schematic diagram illustrating the electronic setup of detection system used to acquire the data.

#### 4.3.1 Detector:

- **Scintillation Detector - Model 802**

The Model 802 Scintillation Detector used in this study is a hermetically sealed assembly which includes a high resolution NaI(Tl) crystal, a photomultiplier tube, an internal magnetic/light shield, an aluminum housing, and a 14-pin connector.

The 802 series of NaI (TI) detectors provide high efficiency and uniform response on both the cylindrical and well configurations. These detectors have a proven record of long term



reliability and stability. The detector used in this study is a 76.2 mm × 76.2 mm (3" × 3") NaI activated with Thallium. The resolution of its crystal is 7.5% at 662 KeV of <sup>137</sup>Cs.

#### **4.3.2 Multi Channel Analyzer (MCA):**

The operation of the multi channel analyzer is based on the principle of converting an analog signal, which is basically the pulse amplitude into an equivalent digital number usually referred to as a channel. After this is done the digital information will be stored in the memory to be displayed on the monitor. This activity is in principle carried out by the Analog to Digital Converter (ADC) (Knoll, 2000). The pulses are collected, sorted according to pulse height in the ADC and a  $\gamma$ -ray spectrum is generated. Therefore the performance of the MCA is primarily dependent on the ADC. The results discussed in this thesis were measured using an MCA (InInspector 2000 DSP) with a PC using the Genie 2000 software program.

#### **4.3.3 InInspector 2000 Portable Spectroscopy Workstation:**

The InInspector 2000 is a high performance, portable spectroscopy workstation based on Digital Signal Processing (DSP) technology. Applications for the InInspector 2000 include all HPGe, NaI and Cd(Zn)Te detector applications common in environmental characterization; nuclear safeguards; decommissioning and decontamination; and in-facility monitoring. Figure 4.2 shows the used portable gamma ray spectroscopy workstation.

Features of InInspector 2000 Workstation include Digital Signal Processing (DSP) technologies, temperature stability for consistent quality operation and low system dead time to reduce counting times and improve measurement accuracy. It also accommodates a wide range of count rates with minimal loss of spectrum resolution. It has an ultra small, ultra light weight package.

Physical specifications include metal and plastic enclosure with a size of 3.8 x 18.5 x 17.3 cm (1.5” x 7.3” x 6.8”) H x W x D. The operating conditions are a temperature of 0 to 50 °C and humidity up to 80%



Figure 4.2: In-situ gamma ray spectroscopy workstation showing the geometry of measurements.

#### 4.3.4 Genie 2000 Basic Spectroscopy Software:

Genie 2000 Basic Spectroscopy Software (Canberra Inc., 2000); is a comprehensive environment for data acquisition, display and analysis in personal computers. It provides independent support for multiple detectors, extensive networking capabilities, windowing interactive human interface and comprehensive batch procedure capabilities.

The full multitasking architecture of Genie 2000 allows the software to overcome the limitations of traditional PC based systems. Multiple independent count procedures can be run for several detectors simultaneously. No procedure is suspended by the activation of another or caused to slow down excessively by software overhead. With Genie 2000, operation is fully independent.

The counting procedure software provides a total environment for the application. In addition to taking standard measurements, the procedures provide a guided user interface for calibration operations, and quality control. Plus, under management level security, setup functions are provided.

When the operator selects sample counting, the system presents a list of available sample types. The sample type embodies the analysis protocol, counting time, parameter entry screen, and geometry. When the sample type is selected, the system prompts the operator for the geometry, then to place the sample in position. Acknowledgment of that screen starts the count and a sample parameter entry screen is presented to the operator. The operator fills in the sample ID and other information that may be essential for the analysis.

This screen can be different for each possible sample type, thus allowing the system to prompt only for the information required by a specific assay. When the acquisition is finished, the spectrum is analyzed automatically and the spectrum, the measurement conditions, and the analysis report are written to disk. The report can also be sent to the screen, to a printer, or to both.

Selection of the quality assurance procedure leads the operator through a step by step operation to count and analyze a check source and store the results in a QA file. Typical systems use  $^{60}\text{Co}$  and  $^{137}\text{Cs}$  check sources and monitor peak position, FWHM and reported peak areas. The system accumulates a historical QA database from which graphical control charts and reports can be created, monitoring the performance of the system.

#### 4.4 Study Area

Abu dies is located in the eastern part of Jerusalem district as shown in Figure 4.3. The records of the Central Weather Station in Jerusalem show that the maximum average temperature is 28.64°C, while the minimum average temperature is 6.12°C (Israeli Meteorological Services, 1994). Bethlehem District on the other hand is located in the southern part of the west bank as presented in Figure 4.4, eight kilometers south of Jerusalem (ARIJ, 1995). On the other hand, the average annual temperature in Bethlehem District is between 22 °C in the summer and 7 °C in the winter.

Gamma ray spectroscopy was carried out in some areas in Jerusalem district and in Bethlehem district. Fifteen locations were investigated for  $\gamma$ -emitting radionuclides in the above named two areas by in-situ  $\gamma$ -ray spectroscopy. Three of these measurements were performed indoor.

Spectra were collected in most cases for 1800 seconds. Some spectra were collected for longer time to insure better statistics and/ or to check for the existence of low level concentrations of anthropogenic radionuclides. Figures 4.3 and 4.4 show the locations of measurements. Table 4.1 describes the characteristics of these locations.

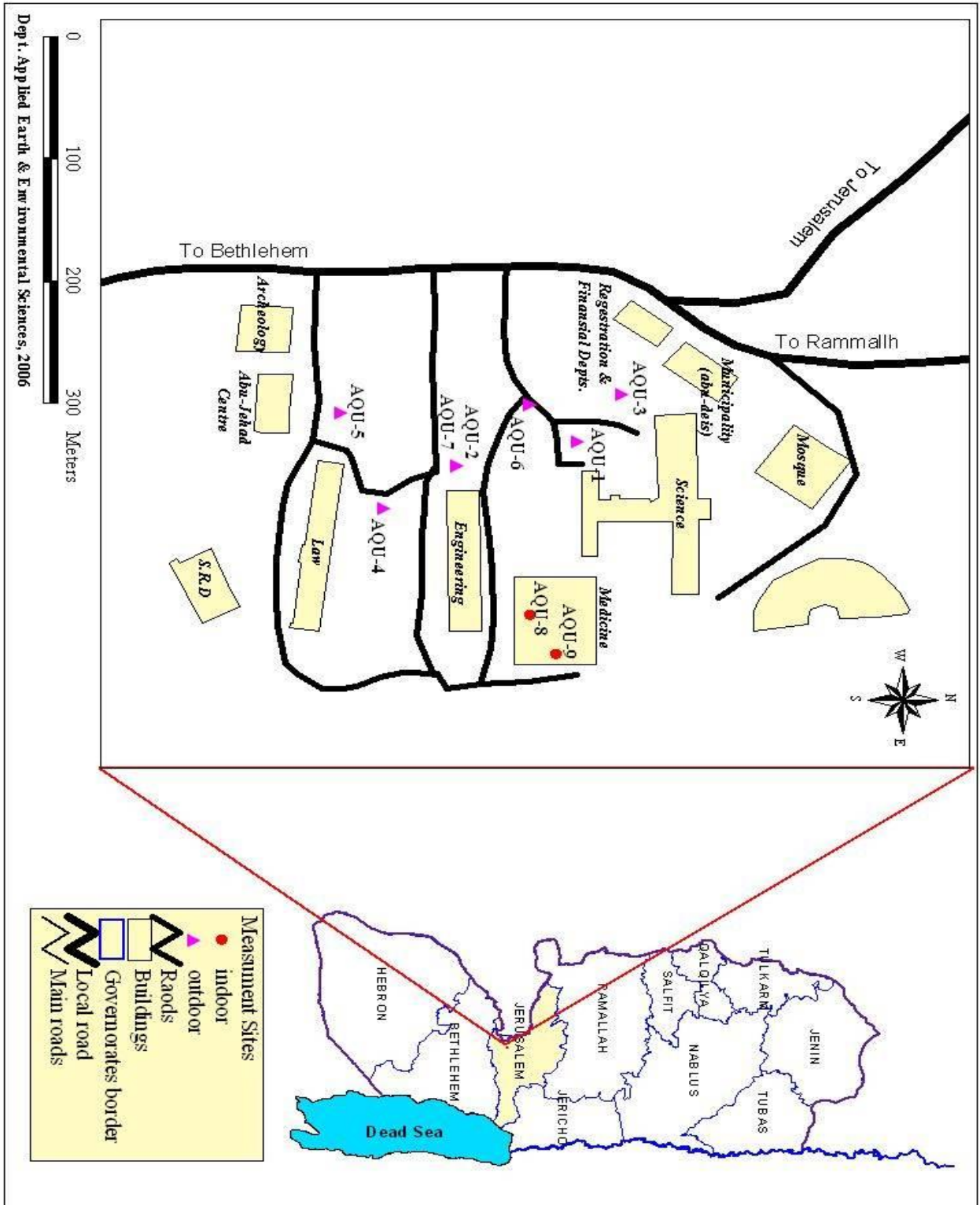


Figure 4.3: Measurement sites at Abu Dies (AQU).



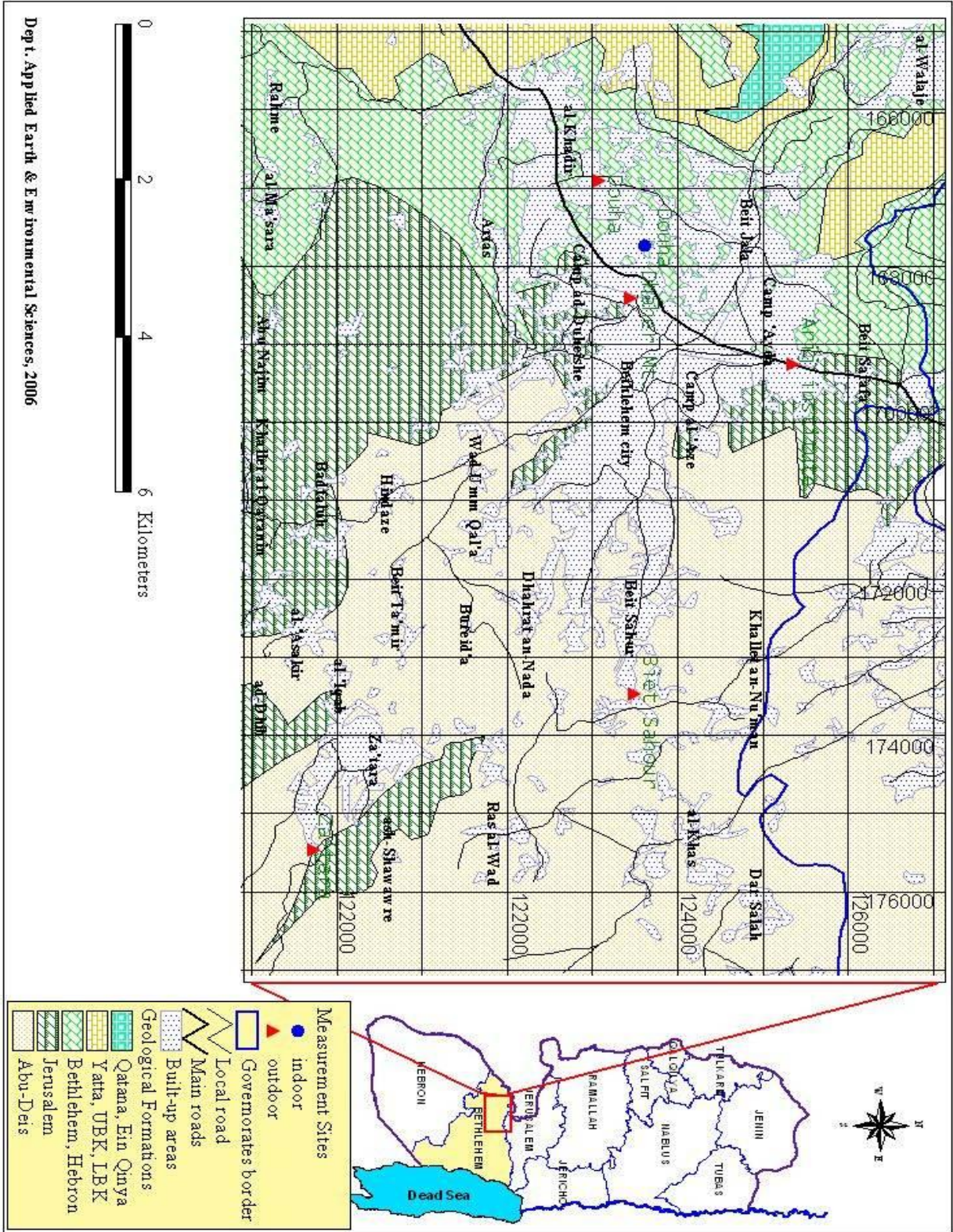


Figure 4.4: Measurement sites at Bethlehem district along with geological formations.

Table 4.1: Measurement locations and area description

<b>Location</b>	<b>Area Description</b>
ARIJ	Semi cultivated soil land with little or non-rocks nearby. No nearby buildings.
Beit Sahour	Uncultivated soil land with small black rock pieces, high landed area.
Dhafer Mt.	Rocky land with small amounts of soil, nearby fracture, and a big deep hole.
Doha City (Indoor)	New building made of concrete and rocks
Doha City	Uncultivated area with no buildings nearby
Za'tara	Uncultivated area with soils and small fragmented rocks, nearby a valley, away from nearest building about 100 m.
AQU-1 (Near College of Science)	Uncultivated grassy land with about 50 m apart from the building.
AQU-2 Near Engineering College	Newly Cultivated soil land, away from the college building about 50 m.
AQU-3 Near University Theatre	Uncultivated soil land, close to trees about 10 m.
AQU-4 In front of College of Law	Uncultivated soil land, between trees.
AQU-5 Beside College of Law	Semi cultivated land with some digging around away up to 30 m.
AQU-6 On University Road	On Road measurement (Street) at the junction of the College of Science and the College of Engineering.
AQU-7 Near Engineering College	Beside Engineering College. After Rain by about 24 hours.
AQU-8 (Indoor) (In-Building) (-1 Floor)	Medical Imaging Dept., New building made of concrete and rocks with some furniture and books around, Open windows.
AQU-9 (Indoor) (Basement)	College of Health Professions , New building made of concrete and rocks, no windows or ventilation is present

#### **4.4.1 Abu Dies Geological Formation:**

Abu Dies formation mainly consists of chalk and chert. It outcrops mainly in the Eastern Slopes of the district. Usually, the chalk is white but in some areas it takes the dark color which is due to the presence of bituminous materials.

#### **4.4.2 Bethlehem Geological Formations:**

The geology of the area, as represented in Figure 4.4, shows the following formations:

1. Limestone and Marl formations.
2. Chalk and Chert formations.
3. Metamorphic rocks and calcium silicate rocks.

Formations such as limestone and sandstone have the lowest radionuclide concentrations. Some shale formations, particularly those containing a significant fraction of organic matter, can possess higher concentrations of radionuclides. Sedimentary rocks, however, tend to accumulate at the top of the crust. Approximately 75% of the surface of the earth is covered by sedimentary rock.

Uranium is prevalent to some degree in all common types of rock and soil. Common rock types contain concentrations of Uranium in the range of 0.5 ppm to 4.7 ppm (NCRP, 1987). These concentrations, however, do not only just refer to  $^{238}\text{U}$  itself, but also to the daughter products inherently contained in the Uranium decay chain. Like Uranium, Thorium is found in all types of rocks and soils. Concentrations of Thorium in common rock types fall between 1.6 ppm and 20 ppm. The concentrations of Thorium in rock and in soil generally exceed that of Uranium.



Sedimentary rock like Shale is comprised of at least 35% clay. A significant fraction of shale contains Potassium. Shale also can adsorb Uranium and Thorium. These radionuclides typically are bound to organic matter in minerals in the rock. The Uranium and Thorium also can be found as precipitates in the material that binds the rock. Quartz is the major mineral that comprises sandstone. Some sandstone contains feldspar in fractions as high as 25%. Feldspar is usually enriched with Potassium. Concentrations of Uranium and Thorium are low in sandstone (Vohra & eds. et. al., 1982). Deposits of these radionuclides have been found at the boundaries of different layers of sandstone.

Carbonate rock is found as limestone or as dolomite, which is formed as a result of the precipitation of materials such as bones and shells from water. Generally, carbonate is almost free of radionuclides. The spaces between carbonate grains, however, can contain some radionuclides. Potassium is very soluble in sea water, and it can remain in these interstitial spaces as the sea water is removed. Thorium also can be present, as it is found in depleted concentrations in sea water. Uranium can be found in limestone as a result of the decay of organic matter deposited where the limestone is located (Beninson et. al., 1977).

## Chapter V

### Results and Discussion

#### Calibration of the Spectrometer

##### 5.1.1 Energy Calibration:

Energy calibration is performed in laboratory and always checked in terrain before and after measurements. Calibration was performed using a point source of  $^{137}\text{Cs}$  with  $\gamma$ -energy of 661.8 KeV; Figure 5.1, and a Petri dish multi  $\gamma$  standard containing the radionuclides of  $^{135}\text{Eu}$ ,  $^{57}\text{Co}$ ,  $^{113}\text{Sn}$ ,  $^{137}\text{Cs}$ ,  $^{54}\text{Mn}$ ,  $^{65}\text{Zn}$ ,  $^{40}\text{K}$  and  $^{125}\text{Sb}$  with activities ranging from 666 Bq – 11.211 KBq. The energy lines corresponding to some of these radionuclides are shown in Figure 5.2.

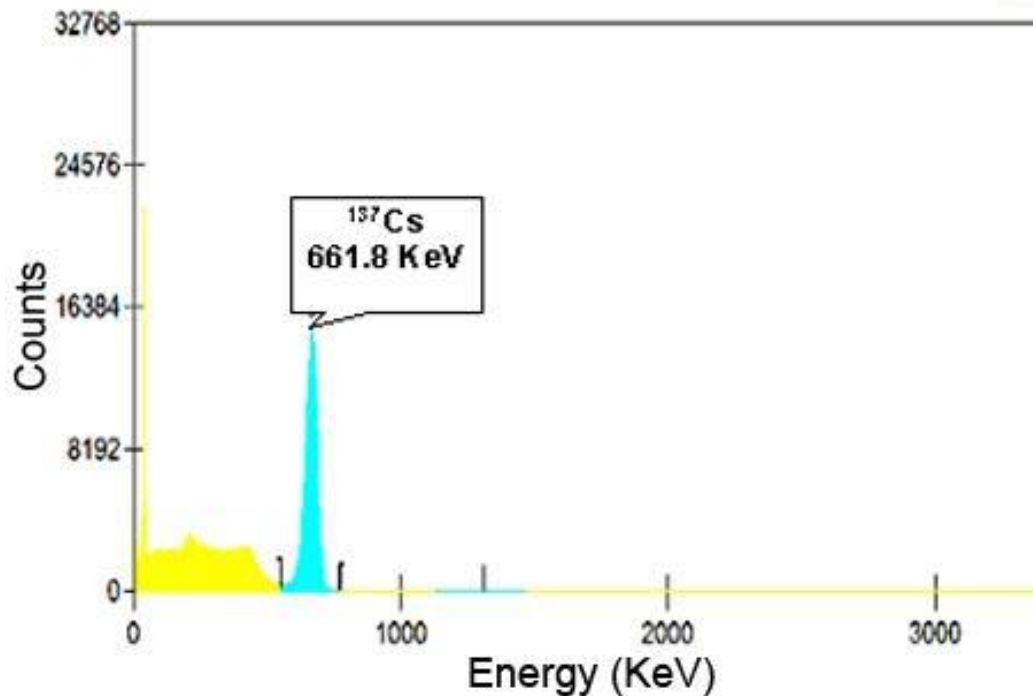


Figure 5.1: Gamma ray spectra of a point source radioactive standard of  $^{137}\text{Cs}$  used for energy and efficiency calibration of the NaI(Tl) 3"× 3" detector.

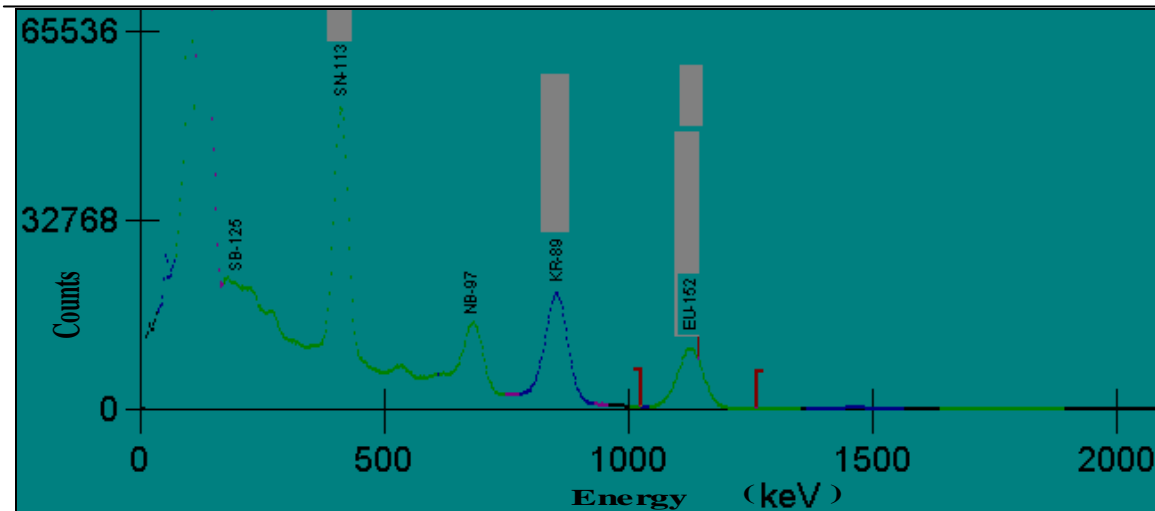


Figure 5.2: Gamma ray spectrum of a mixture of radioactive standards in Petri dish geometry used for energy calibration of the NaI(Tl) 3”× 3” detector.

### 5.1.2 Efficiency Calibration:

The efficiency calibration was performed using Monte Carlo calculations, assuming soil density of  $1.3 \text{ g/cm}^3$  and homogeneously distributed activity of the radionuclides  $^{40}\text{K}$ ,  $^{238}\text{U}$ , and  $^{232}\text{Th}$  within the soil. Monte Carlo calculations are performed in two steps. First: photons of the energies 609.3 KeV, 911.6 KeV and 1460 KeV are randomly generated in a layer of soil at various depths. In the following step, the history and transport of each photon is followed until it interacts with the crystal or escapes from it. Detector response is then calculated from the energy of photons deposited in the NaI(Tl) crystal.

Three soil layers are considered; at depth from 0-5 cm, from 5-10 cm, and from 10-15 cm under the earth surface. Results of efficiency calculations were gained using Monte Carlo simulations and are presented in Figures 5.3 and 5.4. The efficiency value for  $^{208}\text{Tl}$ ; (the decay product of  $^{232}\text{Th}$ ) at the energy of 2615 KeV; is extrapolated from the efficiency curves shown in Figure 5.4.

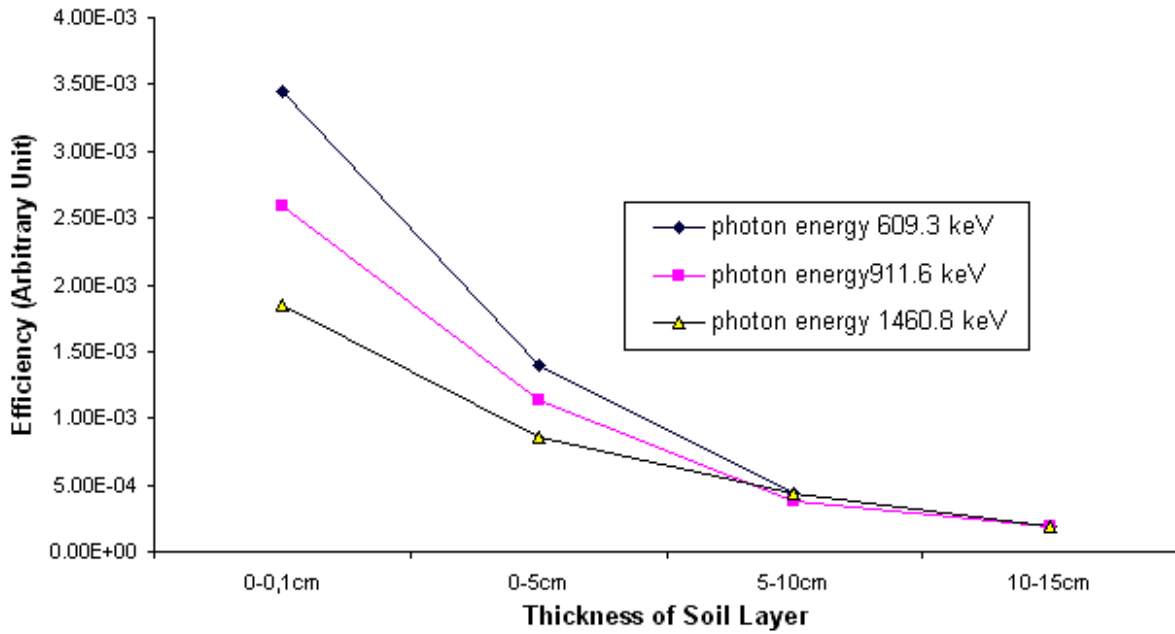


Figure 5.3: Counting efficiency of the used NaI(Tl) detector for various energies and activities of radionuclides homogeneously distributed in an area of 1 m<sup>2</sup> in soil at various depths using Monte Carlo simulation. Detector is located 1 m above soil surface.

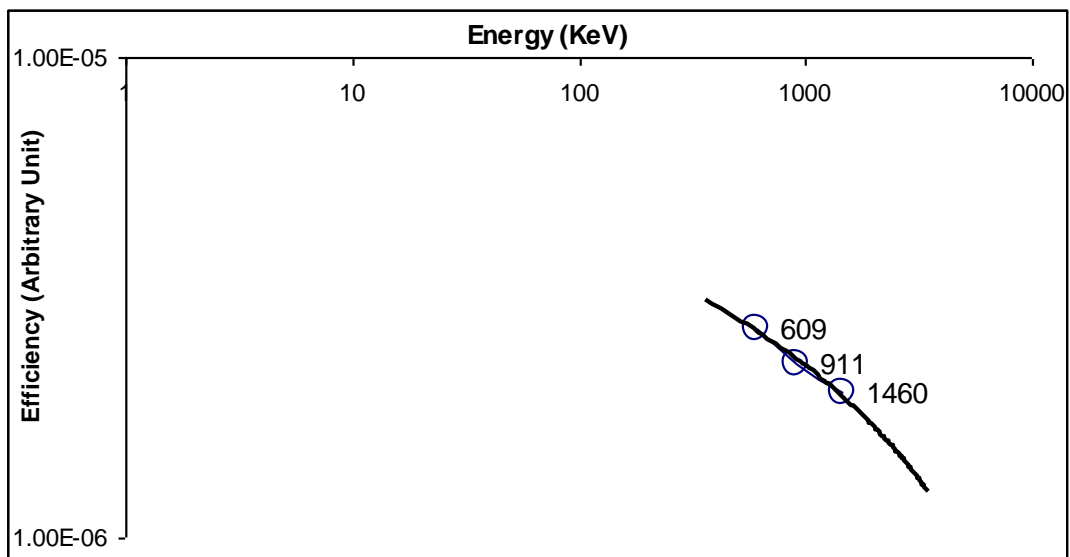


Figure 5.4: Counting efficiency as a function of energy for homogeneously distributed activity in the soil within a circle of 20 meters in radius and depth of 15 cm using Monte Carlo simulation. Soil density is 1.3 g.cm<sup>-3</sup>.

## Qualitative Analysis of Measured Gamma Ray Spectra

Figures 5.5 and 5.6 show a spectrum of  $\gamma$ -rays divided into two parts, low and high energy parts of the spectrum. The spectrum is measured in Beit Sahour and shows the identified radionuclides of  $^{214}\text{Pb}$ ,  $^{214}\text{Bi}$  (decay products of  $^{238}\text{U}$ ),  $^{40}\text{K}$ ,  $^{208}\text{Tl}$  (decay product of  $^{232}\text{Th}$ ) and the anthropogenic  $^{137}\text{Cs}$ . These radionuclides are identified by the  $\gamma$ -energy lines 352 KeV, 609.3 KeV, 1460.8 KeV and 2614.7 KeV respectively.  $^{137}\text{Cs}$  is noticed clear at the energy line of 661.8 KeV and most probably originated from Chernobyl accident.

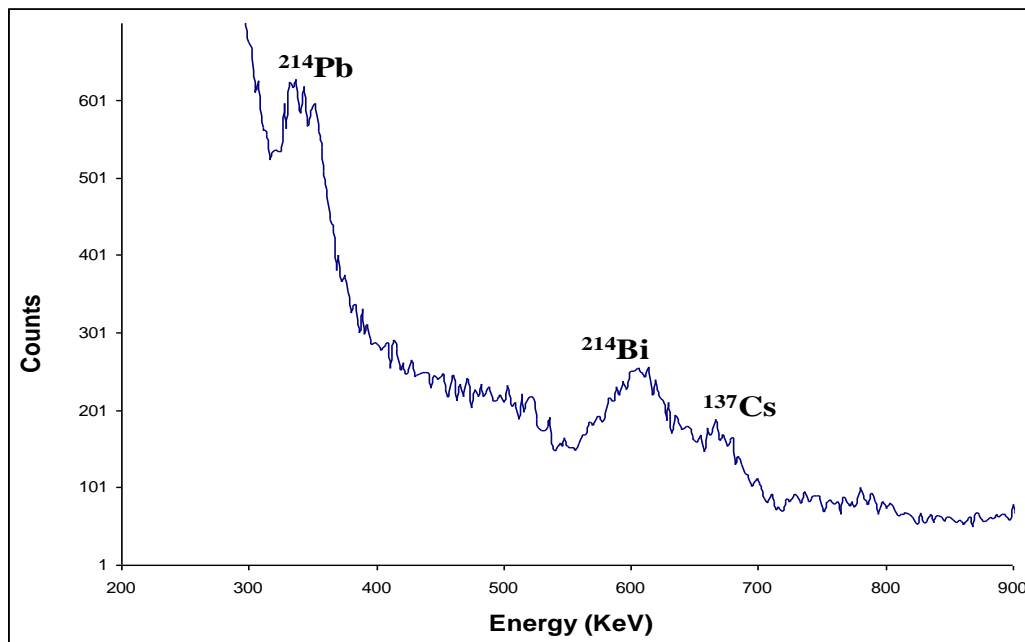


Figure 5.5: Low energy part of a measured  $\gamma$ -ray spectrum showing the identified radionuclides of  $^{214}\text{Pb}$ ,  $^{214}\text{Bi}$  and  $^{137}\text{Cs}$ . This spectrum was collected in Beit Sahour near Bethlehem.

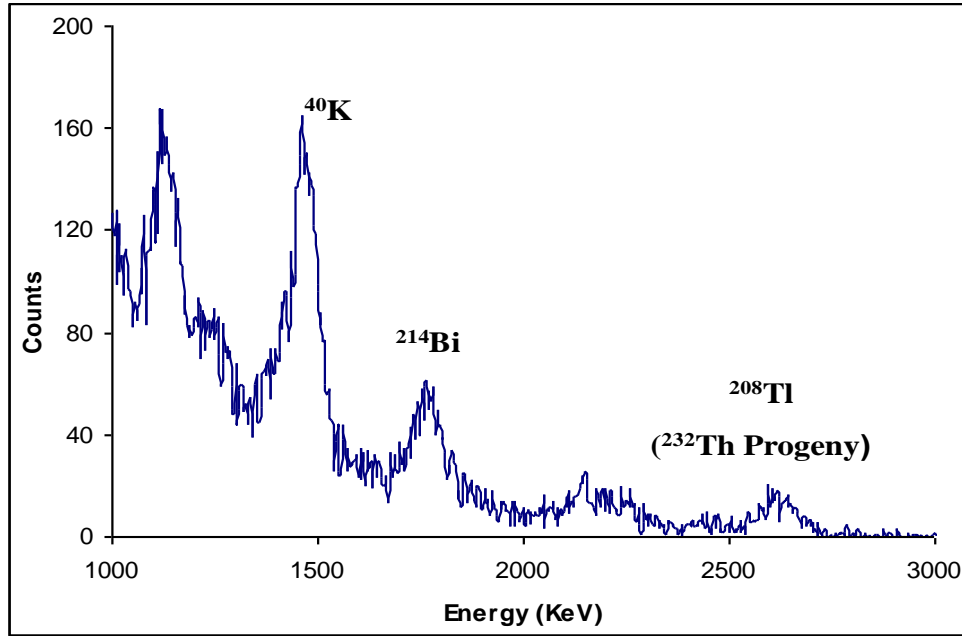


Figure 5.6: High energy part of a measured  $\gamma$ -ray spectrum collected in Beit Sahour showing the peaks which represent  $^{40}\text{K}$ ,  $^{214}\text{Bi}$  and  $^{208}\text{Tl}$  energy lines.

The presence of  $^{137}\text{Cs}$  from Chernobyl has been reported in some studies in Syria, Jordan, Saudi Arabia and other Middle East countries. Although the amount of  $^{137}\text{Cs}$  is very small in the measured spectrum, this radionuclide has been identified because of the good resolution of the spectrometer and the accuracy of energy calibration.

$^{137}\text{Cs}$  is also found at Doha City, but in smaller amounts than in Beit Sahour as indicated in Figure 5.7. The amount is so small that better identification and may be also determination of its content in soil can be achieved only using spectrometer with high resolution and sensitivity as well.

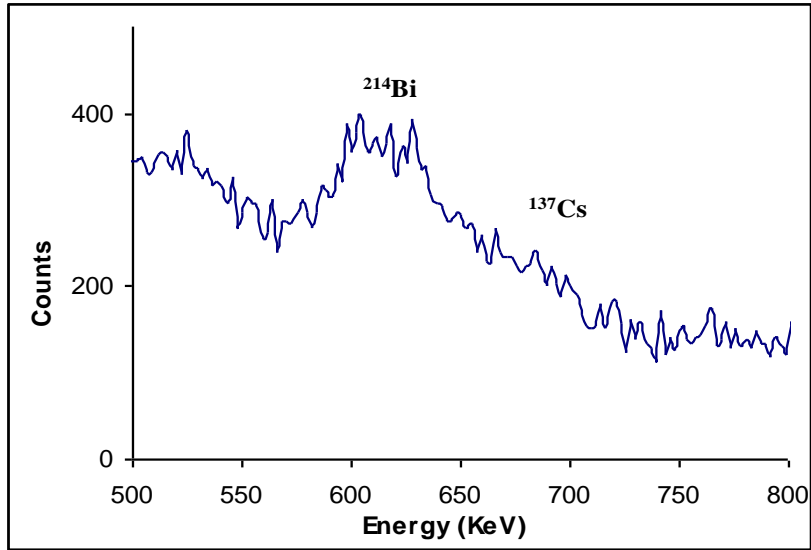


Figure 5.7: Part of  $\gamma$ -ray spectrum measured in Doha City indicating the presence of trace amounts of anthropogenic  $^{137}\text{Cs}$ .

$^{137}\text{Cs}$  is a man-made radionuclide produced through nuclear fission. It has very high fission yield, and has a 30.1 years half-life. The  $^{137}\text{Cs}$  parent isotope decays to produce  $^{137\text{m}}\text{Ba}$  with a 2.55 min. half-life which in turn decays, generating a 661.8 KeV gamma ray emission. The Decay process of  $^{137}\text{Cs}$  is shown in Figure 5.8. From a non-radiological hazards point of view, no potential health effects are known for Cesium. However, large oral doses of the material may cause gastrointestinal disturbances.

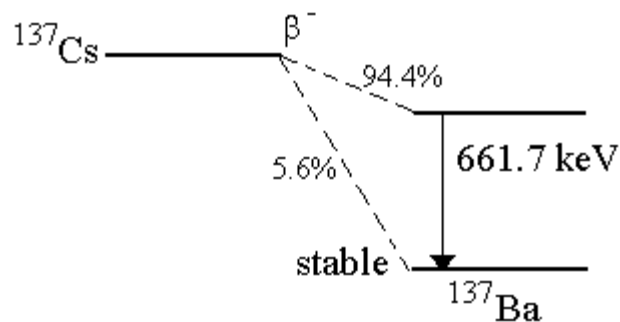


Figure 5.8: A Schematic Diagram of the Radioactive Decay of  $^{137}\text{Cs}$  (Norman E. and Rech G., 1996).

A large amount of  $^{137}\text{Cs}$  was released into the atmosphere from nuclear tests in early 1950's and 1960's, and from nuclear accidents in the past, mainly Chernobyl. From the radiological point of view,  $^{131}\text{I}$  and  $^{137}\text{Cs}$  are the most important radionuclides to consider, because they are responsible for most radiation exposure received by the general population. Radioactive contamination of the ground with  $^{137}\text{Cs}$  was found to some extent in practically every country of the northern hemisphere (EGE, 2005).

### Indoor and Outdoor Measurements

Comparison is made between outdoor and indoor measurements in two locations: Figures 5.9 and 5.10 illustrate the differences in the intensity of low energy parts of a  $\gamma$ -ray spectra measured outside and inside AQU building at Abu Dies campus and at Doha city.

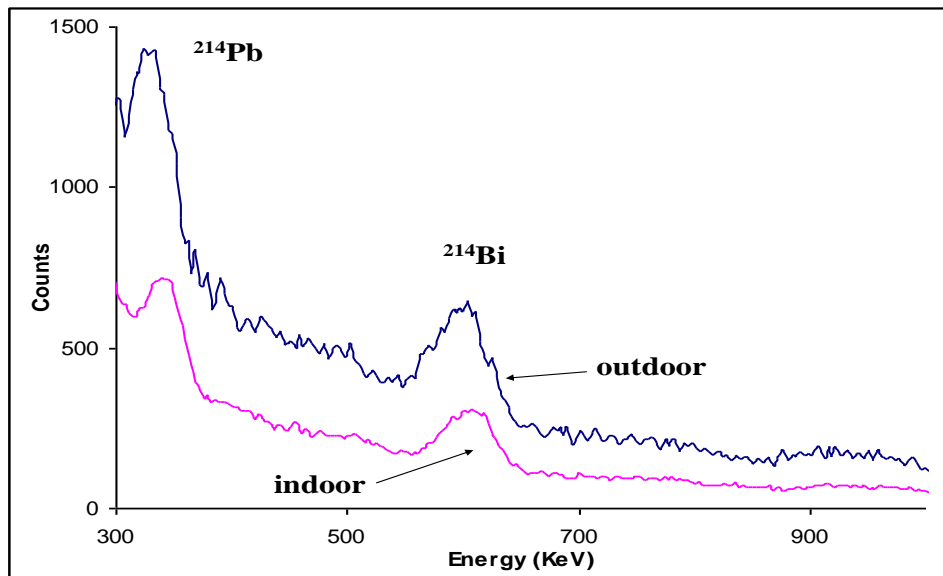


Figure 5.9: Differences in  $\gamma$ -ray spectrum at low energies measured outdoor and indoor at Al-Quds University site.



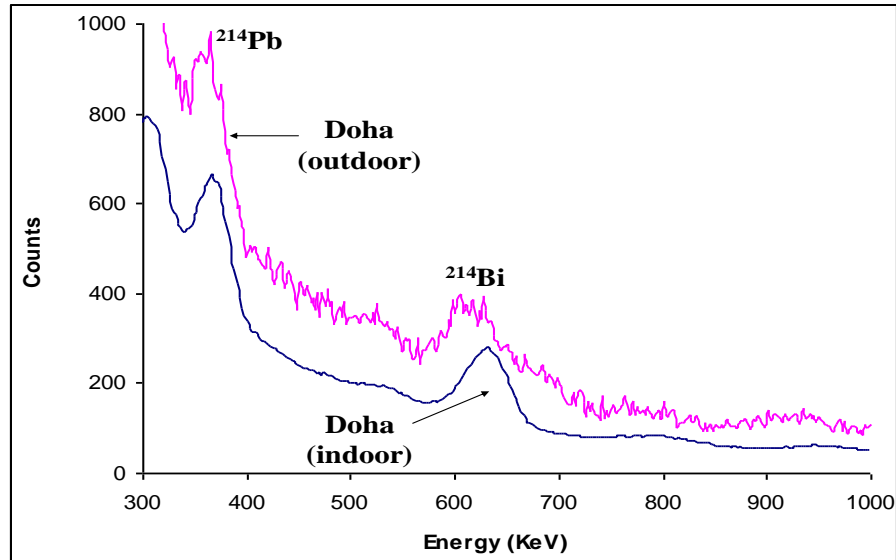


Figure 5.10: Differences in  $\gamma$ -ray spectrum at low energies measured outdoor and indoor at Doha City site.

Figure 5.11 illustrates the differences in the intensity of high energy parts of a  $\gamma$ -ray spectra measured inside AQU building at Abu Dies campus and at Doha city near Bethlehem..

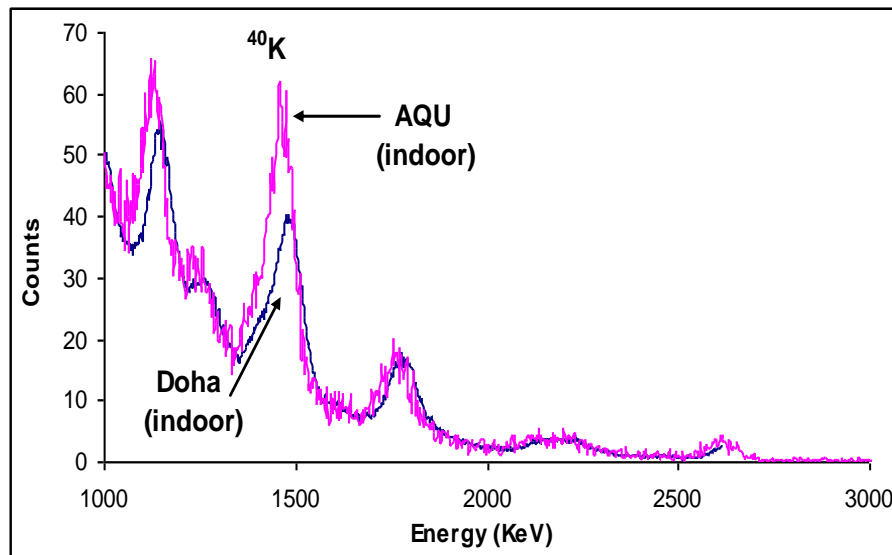


Figure 5.11: Differences in  $\gamma$ -ray spectrum at high energies measured indoor at Al-Quds University and at Doha City sites.

It is obvious that identified radionuclides and the area below their peaks (their amounts); are less in indoor than outdoor. This is very clear and well visualized at the peaks of  $^{214}\text{Pb}$ ,  $^{214}\text{Bi}$ ,  $^{40}\text{K}$  and  $^{208}\text{Tl}$ . Several factors contribute to the variability of indoor radionuclide concentrations. Meteorological factors can play an important role in the transportation of radionuclides from place to another or from outside to inside buildings. Areas with high concentrations in groundwater can lead to high concentrations of indoor radon. The choice of building materials also has the influence on changing radionuclide concentration.

The highest ratio of peak areas of identified radionuclides measured indoor and outdoor was determined to be 2 in Doha City and 2.8 in AQU. This ratio ranging from 1 to 2.8 has an average of 1.8, was found to be in correlation with the ratio of outdoor to indoor gamma dose rates that varies between 0.8 to 2 with an average value of 1.3 (Guy, 1988). Table 5.1 presents the radionuclide ratios of outdoor to indoor count rates at different locations.

Table 5.1: Outdoor to indoor peak area ratios corresponding to  $^{40}\text{K}$ ,  $^{214}\text{Bi}$  and  $^{208}\text{Tl}$  at Al-Quds University and Doha City sites.

Radionuclide	Location	Ratio
$^{40}\text{K}$	Al-Quds University	2.8
	Doha	2
$^{214}\text{Bi}$	Al-Quds University	1.34
	Doha	1.2
$^{208}\text{Tl}$	Al-Quds University	1.9
	Doha	2

Figure 5.11 shows in general higher concentrations of radionuclides measured indoor. This indicates that building materials used in Abu Deis site have higher concentrations of radioactivity.

## Quantitative Analysis of Identified Radionuclides

Terrestrial radionuclides are distributed throughout the crust of the earth according to geological formation present in the area of measurement. Background count rates include contributions from cosmic rays and background radiation in the detector material itself. Background count rate can be determined using upward looking detectors or by measuring over bodies of water. In this study, background spectrum was measured using upward looking detector and then subtracted from the measured spectra at each location. Figure 5.12 shows the background spectrum measured using the geometry of upward looking detector. Detector face is turned upward at 1 m height from the ground surface. The activity of individual radionuclides is calculated according to the following equation:

$$A = \frac{N}{T \cdot \epsilon \cdot Y} \quad (1)$$

Where A: Activity of Radionuclide of interest (Bq)

N: Net Peak Area;

T: Counting Time;

$\epsilon$ : Detection Efficiency;

Y: Yield (Number of Photons per Disintegration).

The activity per kilogram of a radionuclide of interest is derived from the overall activity determined for a circle of 20 meters in radius and depth of 15 cm under the ground surface assuming soil density of  $1.3 \text{ g.cm}^{-3}$ . This area represents approximately 97% of the activity detected by the detector placed 1 meter above the ground surface.

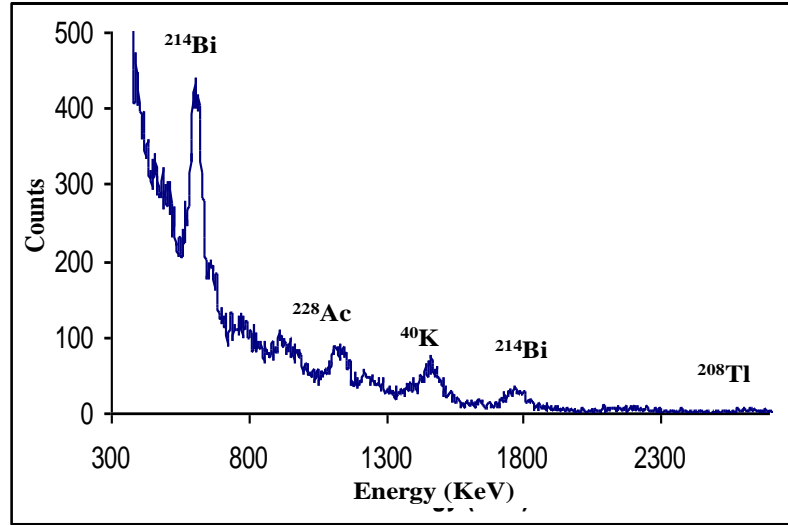


Figure 5.12: Background spectrum measured using upward detector geometry at 1 m height above the ground level at AQU.

It is noticed from the background spectrum that radionuclides emitting  $\gamma$ -radiation of higher energies from inside the earth crust (that are  $^{228}\text{Ac}$ ,  $^{40}\text{K}$ ,  $^{214}\text{Bi}$  and  $^{208}\text{Tl}$ ) are not so significant in the background spectrum. On the other hand  $^{214}\text{Bi}$  at the energy of 609.3 KeV has significant peak in the background. This can be explained by the higher counting efficiency for  $^{214}\text{Bi}$  at 609.3 KeV and also the existence of atmospheric Radon of which  $^{214}\text{Bi}$  is a progeny.

As soon as the amount of  $^{40}\text{K}$  is determined, the amount of natural Potassium is known because  $^{40}\text{K}$  constitutes about 0.012% of natural Potassium. Also,  $^{238}\text{U}$  and  $^{232}\text{Th}$  mass concentrations in ppm can be determined. Activity concentrations of radionuclides of  $^{40}\text{K}$ ,  $^{214}\text{Bi}$  and  $^{208}\text{Tl}$  given in ( $\text{Bq.kg}^{-1}$ ), ppm for eU and eTh; are shown in histograms 5.13, 5.14, 5.15 and in table 5.2. The average content for these radionuclides in Palestinian soils is given in table 5.3.

In order to convert the radionuclide concentration of  $^{40}\text{K}$ ,  $^{238}\text{U}$  and  $^{232}\text{Th}$  to specific activity, the relationship is as follows (IAEA, 1989):

$$1\% \text{ K in rock} = 313 \text{ Bq/kg } ^{40}\text{K}$$

$$1 \text{ ppm U in rock} = 12.35 \text{ Bq/kg } ^{238}\text{U}$$

$$1 \text{ ppm Th in rock} = 4.06 \text{ Bq/kg } ^{232}\text{Th}$$

Table 5.2: Activity concentration of identified radionuclides.

Location	$^{214}\text{Bi}$ Activity (Bq/Kg)	$^{208}\text{Tl}$ Activity (Bq/Kg)	$^{40}\text{K}$ Activity (Bq/kg)	ppm eU	ppm eTh
AQU-7 (After Rain)	9	15	304	1	4
AQU-2 (Before Rain)	14	19	3	1	5
AQU-5	7	20	350	1	5
AQU-4	6	5	36	1	2
AQU-6	8	33	36	1	9
AQU-1	34	12	13	3	3
AQU-3	44	19	454	4	5
ARIJ	5	3	192	1	1
Beit Sahour	24	3	127	2	1
Doha City	29	24	325	2.4	6
Dhaher Mt.	1	2	88	<1	1
Za'tara	27	10	197	2.2	2

Table 5.3:  $^{40}\text{K}$ ,  $^{238}\text{U}$  and  $^{232}\text{Th}$  content in Palestinian soil.

Radionuclide	$^{40}\text{K}$ (Bq/kg)	$^{214}\text{Bi}$ (Bq/kg)	$^{208}\text{Tl}$ (Bq/kg)	eU (ppm)	eTh (ppm)
Content in Soil (range)	3 - 454	1 - 44	1 - 33	1 - 4	1 - 9
Average	$177 \pm 26$	$17 \pm 2.5$	$14 \pm 2.1$	$2 \pm 0.3$	$4 \pm 0.6$

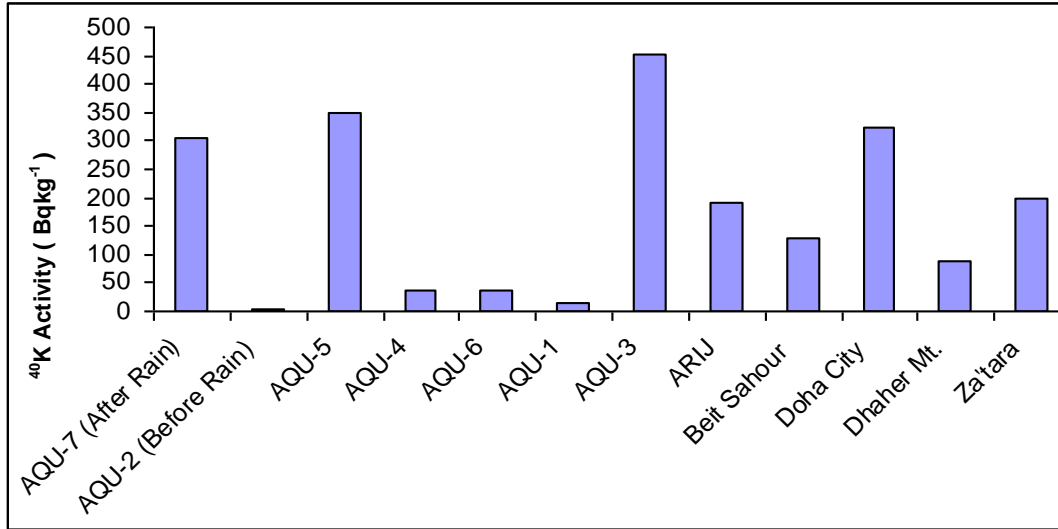


Figure 5.13: Distribution of  $^{40}\text{K}$  throughout measurement locations.

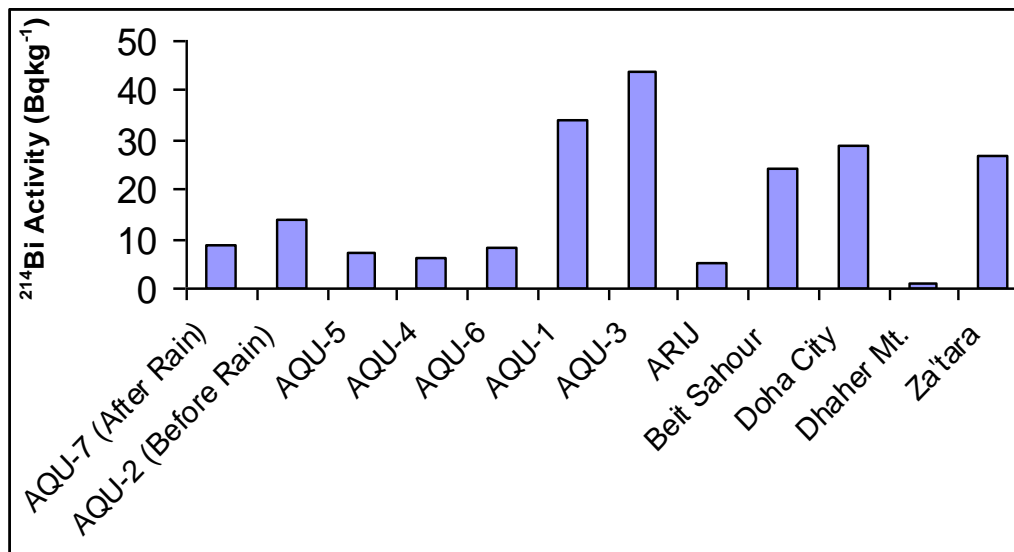


Figure 5.14 Distribution of  $^{214}\text{Bi}$  throughout measurement locations.

The count rates illustrated in Figure 5.15 show that  $^{214}\text{Bi}$  which is a  $^{222}\text{Rn}$  progeny, has its higher count rate in (AQU-1) and (AQU-3). It is also clear from the histogram that  $^{214}\text{Bi}$  has decreased after rain as shown from (AQU-2) and (AQU-7), which were taken before and after rain for the same location. Another case is shown in Figure 5.20, where the increase of  $^{214}\text{Bi}$  count rate in the basement of the College of Health Professions; (AQU-9), when

compared to the Medical Imaging Department which is located above this basement; (AQU-8); due to the accumulation of  $^{222}\text{Rn}$  gas in the basement because no ventilation or windows are present as will be explained in section 5.6. Activity concentrations of identified radionuclides could not be determined for AQU-8 and AQU-9; because the efficiency calibration was only simulated for outdoor measurements.

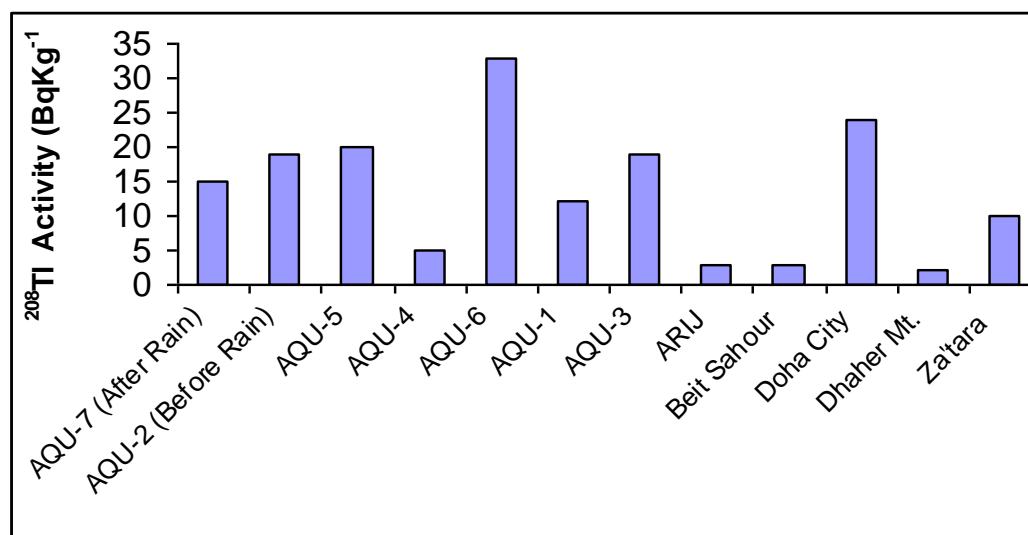


Figure 5.15: Distribution of  $^{208}\text{Tl}$  (the decay product of  $^{232}\text{Th}$ ), throughout measurement locations.

The ratio of eTh/eU is used for analyzing the survey data and to determine which sites may be relatively enriched or depleted in one of the radionuclides due to hydrothermal or hydrological processes. The relative distribution and ratios of eTh and eU are shown in table 5.4 and in Figures 5.16 and 5.17.

Table 5.4: Ratios of concentrations of U and Th.

Location	ppm eU	ppm eTh	U/Th	Th/U
AQU-7 (After Rain)	1	4	0.25	4
AQU-2 (Before Rain)	1	5	0.2	5
AQU-5	1	5	0.2	5
AQU-4	1	2	0.5	2
AQU-6	1	9	0.11	9
AQU-1	3	3	1	1
AQU-3	4	5	0.8	1.25
ARIJ	1	1	1	1
Beit Sahour	2	1	2	0.5
Doha City	2.4	6	0.4	2.5
Dhaher Mt.	1	1	1	1
Za'tara	2.2	2	1.1	0.9

Typical ratio of Th/U in the earth crust is about 3. The ratio of Th/U in this study is about 2.2.

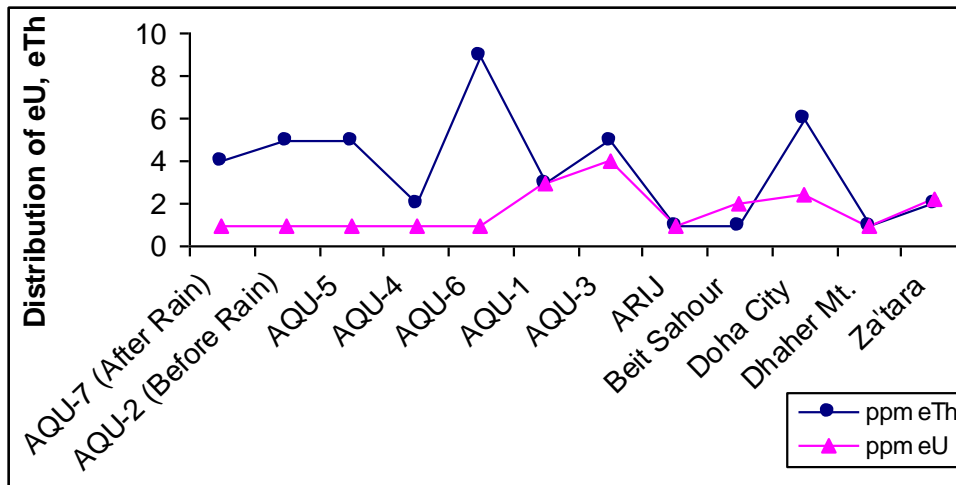


Figure 5.16: Relative distribution of eU and eTh throughout measurements sites.

The ratio of Th/U can be used as an indicator to the nature of metals present in the soil in the region of interest. If  $Th/U \geq 1$ , this indicates the presence of alkaline metals. If  $Th/U < 1$ , non-alkaline metals are present.



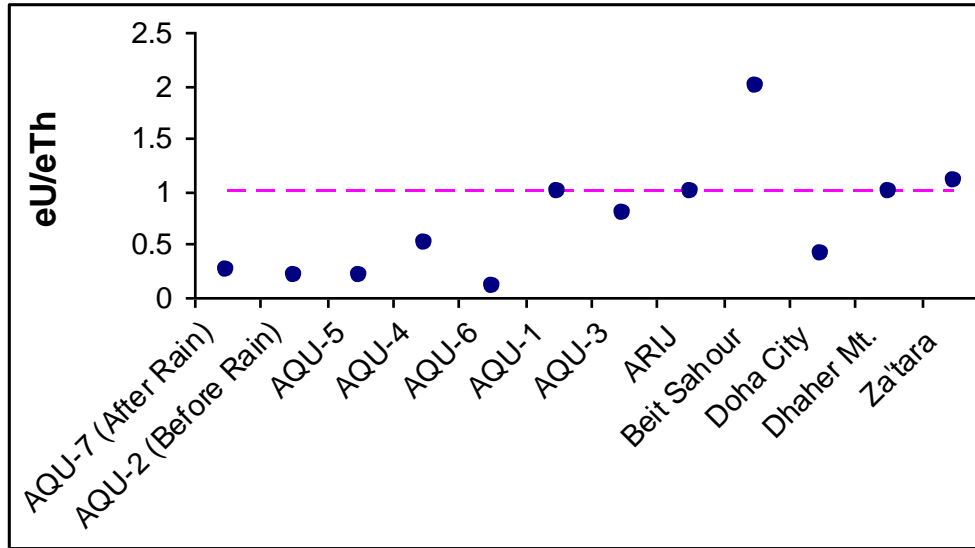


Figure 5.17: Ratios of eU / eTh throughout measurements sites.

### Effect of Rain

Rain is known to be one of major factors affecting the dose rate coming from top soils. That's why during wet weather, attenuation due to water logging in the topsoil can reduce gamma dose rate by up to 20%. Also, snow cover of 20 cm will reduce the gamma dose rate from the soil surface by one half. A comparison between  $\gamma$ -spectra measured before and after rain is shown in Figures 5.18 and 5.19. Both spectra were collected at the same location at Al-Quds University campus.

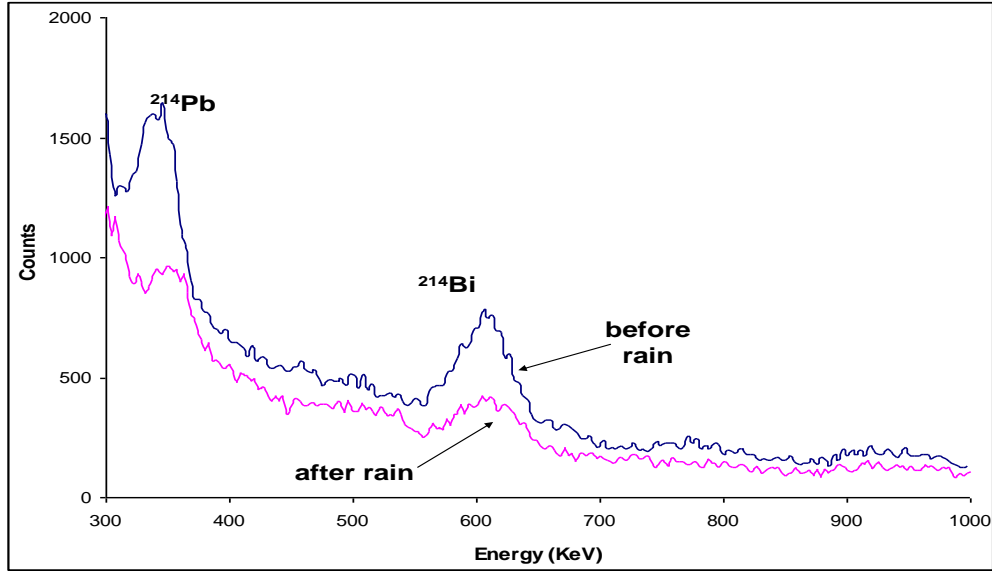


Figure 5.18: Low energy parts of  $\gamma$ -ray spectra measured at the same location (College of Engineering) before and after rain representing  $^{214}\text{Pb}$  and  $^{214}\text{Bi}$  (decay products of  $^{238}\text{U}$ ).

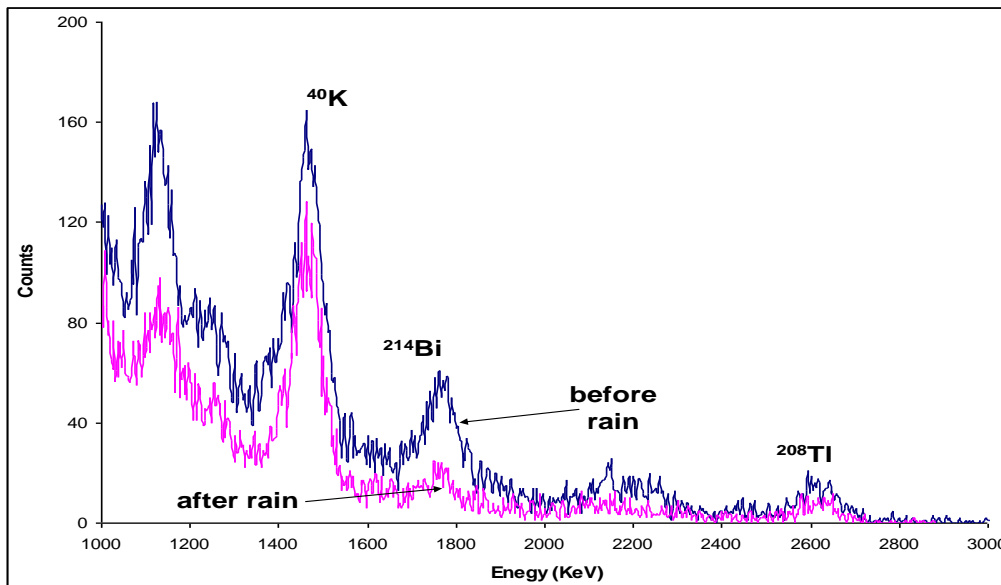


Figure 5.19: High energy parts of  $\gamma$ -ray spectra measured at the same location (College of Engineering) before and after rain representing  $^{40}\text{K}$ ,  $^{214}\text{Bi}$  (decay product of  $^{238}\text{U}$ ) and  $^{208}\text{Tl}$  (decay product of  $^{232}\text{Th}$ ).

Ratios of intensities of  $\gamma$ -rays emitted from the radionuclides  $^{40}\text{K}$ ,  $^{214}\text{Bi}$  and  $^{208}\text{Tl}$  measured before and after rain are determined to measure the effect of rain on  $\gamma$ -spectra attenuation. These ratios are summarized in table 5.6. It is evident from Figures 5.18 and 5.19 that low energy part of the spectrum is more affected by rain. The difference is clear in the peak representing  $^{214}\text{Pb}$ . In general, high energy part of the spectrum is less influenced by rain. Except in the case of  $^{214}\text{Bi}$  (decay product of  $^{238}\text{U}$ ), although it has higher energy than  $^{40}\text{K}$  which is less attenuated by rain than  $^{214}\text{Pb}$ . This is again the effect of gaseous  $^{222}\text{Rn}$  escaped from the soil. Rain fills the pores in the soil and thus prevents Radon from escaping and therefore contributing to the irradiation of the detector. The table shows that rain does not play an important role in the case of  $^{40}\text{K}$  and  $^{208}\text{Tl}$  determination. These radionuclides have enough energy to penetrate the water filled pores and reach the detector.

Table 5.5: Attenuation ratios resulting from the effect of rain

Radionuclide	Count Rate ( $\text{s}^{-1}$ )		Ratio
	before Rain	after Rain	
$^{40}\text{K}$	1.25	1.17	1.06
$^{214}\text{Bi}$	0.82	0.57	1.43
$^{208}\text{Tl}$	0.57	0.45	1.2

### Effect of Radon gas on indoor measurements

Indoor measurements were performed at AQU in two locations representing two floors of the building of the college of medicine. One spectrum was collected on the first floor at well ventilated room; the second was in the basement in a closed non-ventilated room. Comparison between the two measurements is shown in Figure 5.20.

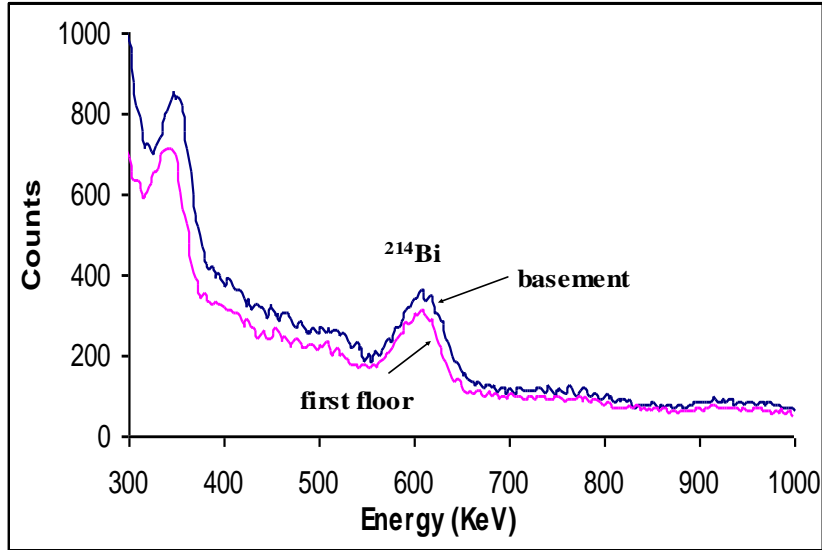


Figure 5.20: Comparison between  $\gamma$ -ray spectra measured indoors at AQU in the first floor and in the basement.

Figure 5.20 shows a higher count rate in the basement for  $^{214}\text{Bi}$  at the energy of 609.3 KeV, which is a decay product of  $^{222}\text{Rn}$ . Here the effect of Radon gas is evident, since closed non-ventilated areas have higher concentrations of Radon.  $^{214}\text{Bi}$  is higher in the basement than in the first floor by about 15%.

### Sensitivity of the Detection System

The sensitivity of the detection system was estimated by calculating the minimum detectable amount of radionuclides of interest using the following equation (Lahham and Fülöp, 1996):

$$MDA = \frac{q^2 + 2q\left[\left(\frac{N}{2n}\right)\left(1 + \frac{N}{2n}\right)\left(\sum B_i + \sum B_j\right) + I + \sigma_i^2\right]^{\frac{1}{2}}}{T \cdot \epsilon \cdot Y \cdot m} \quad (2)$$

Where:

$q \equiv$  the quantile of normal distribution; (For confidence level of 68.27%,  $q$  is 0.5),

$\varepsilon \equiv$  the detector efficiency,

$Y \equiv$  the yield,

$T \equiv$  the time of measurement,

$N \equiv$  the number of channels in the peak of interest,

$n \equiv$  the number of background channels on both sides of the peak of interest,

$B_i \equiv$  the sum of counts in the  $i^{\text{th}}$  channel,

$B_j \equiv$  the sum of counts in the  $j^{\text{th}}$  channel,

$I \equiv$  the net peak area and

$\sigma \equiv$  the error of determination of area  $I$ . Figure 5.21 illustrates the method used for MDA determination.

$m \equiv$  mass of soil layer “seen” by the detector.

Minimum detectable activity (MDA) was calculated for  $^{40}\text{K}$  and found to be around  $1 \text{ Bqkg}^{-1}$ .

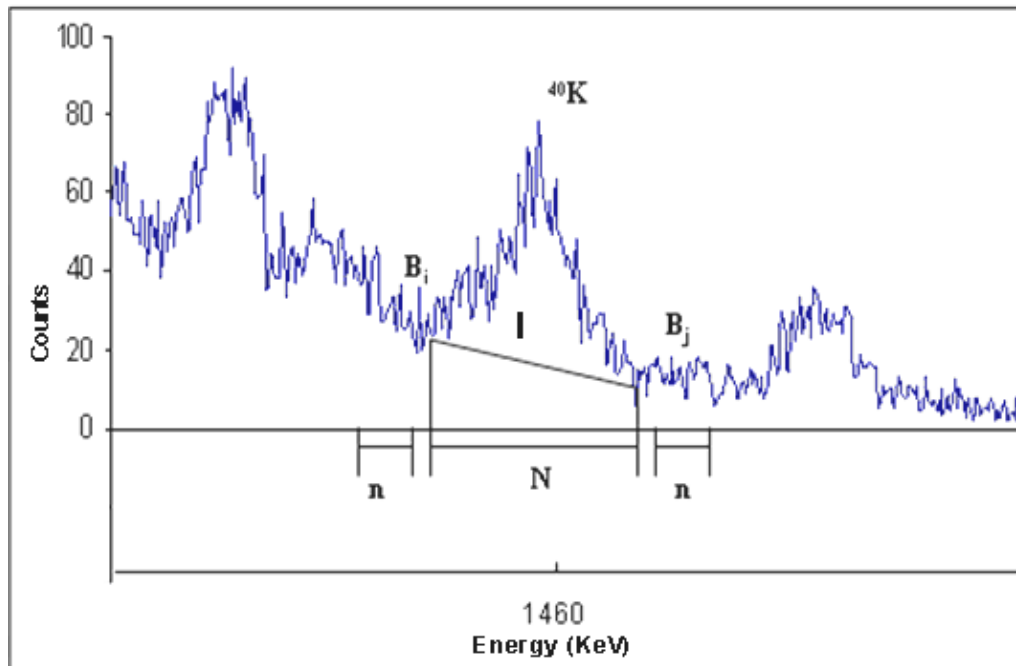


Figure 5.21: Method of MDA determination for  $^{40}\text{K}$ .

## Conclusions and Recommendations

The importance of this study stems from the following: first; it is the first study of its type in Palestine; and it has established a good basis for environmental radioactivity investigation. The system used for measurements provided very good performance in terms of quantitative and qualitative study of  $\gamma$ -ray spectra emitted from the earth crust. It is well calibrated, easy to use and to be positioned in various terrain conditions. Even though, the resolution of the scintillation detectors is a disadvantage in comparison with high resolution Ge spectrometers, data resulted from this work showed that, these detectors are still applicable in  $\gamma$ -ray spectroscopy, mainly when appropriate software for spectra analysis is available. Furthermore, the high sensitivity of scintillators made it possible to collect gamma ray spectra with good statistics in short time periods.

All investigated locations were characterized with natural radioactivity coming from the decay products of  $^{238}\text{U}$ ,  $^{232}\text{Th}$  and  $^{40}\text{K}$  except in two locations of Biet Sahour and Doha city in Bethlehem district where the anthropogenic  $^{137}\text{Cs}$  has been identified in very small concentrations which could not cause any health effect for the Palestinian population.

Measurements performed before and after rain showed that, rain affect mainly the low energy part of the spectrum at energies corresponding to the decay products of Radon. Also, the high energy peak of  $^{214}\text{Bi}$  ( $E_{\gamma} = 1764.5 \text{ KeV}$ ) is significantly deformed by rain. Care should be taken when using this energy for the estimation of the  $^{238}\text{U}$  concentration in soil. Indoor measurements indicated that, materials used for the construction of Al-Quds University buildings contain higher concentrations of naturally occurring radionuclides.

Having information about the concentrations of naturally occurring radionuclides is of particular importance in environmental, geological and geophysical studies. This work provides good opportunity to investigate the nature and composition of soil elements. Terrestrial radiation originates from the decay of radionuclides present in all natural substances; in soil, air and water. These radionuclides can enter the human body via inhalation or ingestion and consequently externally and internally irradiate people. The study of Potassium in the human body is very important for many applications. Its content in the body depends on geographic locations. Therefore, knowing the concentrations of radioactive Potassium in geographical locations is valuable for the study of Potassium content in Man.

Recommendations can be summarized as follows:

1. Increase the number of measured locations over the West Bank and combine measurements with  $\gamma$ -dose rate surveys to construct the radiation map of the country.
2. Application of the results obtained in this thesis in geological and geophysical investigations.
3. Establish a laboratory for gamma ray spectroscopy to be able to analyze soil samples and radioactivity of building materials used in house constructions in Palestine.
4. Develop an appropriate software to be used for instruments calibration to avoid the need for radioactive standards. Monte Carlo simulation is found to be a good tool for this purpose.
5. Inform and promote common policies and practices in Palestine for the management and control on natural sources of exposure.

## References

- Applied Research Institute – Jerusalem (1995), Environmental Profile for The West Bank, Bethlehem District, Volume 1.
- Canberra Inc., (2000). Genie 2000 Basic Spectroscopy Software, V. 3.0, Meriden, CT 06450, U.S.A. ([www.canberra.com](http://www.canberra.com)).
- Canberra Inc., (2005). In-situ Gamma Spectroscopy Systems for Soil and Surface Activity Measurements. U.S.A. <http://www.canberra.com/literature/973.asp>, (accessed 6/11/2005).
- Charbonneau, B.W., & Darnley, A.G., (1970). Radioactive precipitation and its significance to high sensitivity gamma ray spectrometer surveys. Geological Survey of Canada, Paper 70-1, part B, 32-36.
- D. J. Beninson, et. al., (1977). “Dosimetric Implications of the Exposure to the Natural Sources of Irradiation,” Simposio Internacional Sobre Areas De Elevada Radioatividade Natural, (Rio de Janeiro, Brazil: Academia Brasileira de Ciencias).
- Defra (1999), Radioactivity and Environmental Protection. U.K. <http://www.defra.gov.uk/environment/radioactivity/background/> (accessed 4/11/2005).
- Eisenbud M., Gesell T., .Environmental Radioactivity: from natural, industrial and military sources., fourth edition, Academic press, publishers San Diego (1997).
- Expert Group “Environment” (EGE), Environmental Consequences of the Chernobyl Accident and Their Remediation: Twenty Years of Experience. Report of the UN Chernobyl Forum, August, 2005.
- Fugro, (2001), Airborne Gamma-Ray Spectrometry, Australia <http://www.fugroairborne.com.au/services/radiometrics/> (accessed 6/11/2005).



- Giffin N., (1996). Possible pathways of radioactivity in the Ecosystem of Man. [www.triumf.ca/safety/rpt/rpt\\_4/node6.html](http://www.triumf.ca/safety/rpt/rpt_4/node6.html) (accessed 14/6/2006).
- Golikov V.YU., Balonov M. I., Jacob P. (2002), External exposure of the population living in areas of Russia contaminated due to the Chernobyl accident, *Radiation Environmental .Biophysics.*, 41, 185–193.
- Grasty, R.L. (1998). Airborne gamma-ray spectrometer surveying. Airborne Geophysics, I.A.G.E. Week-end course, 16th&17th May, 1998 at Galway Bay Golf & Country Club Hotel, Oranmore, Ireland.
- Grasty, R.L., Cox, J.R., (1997). A car-borne gamma ray spectrometer system for natural radioactivity mapping and environmental monitoring. In RESUME 95, Rapid Environmental Surveying Using Mobile Equipment, Report, Nordic Nuclear Safety Research Secretariat, 71- 90.
- Guy, S. (1988). An overview Of Natural Background Radiation Sources, Part 1: External Sources of Radiation Exposure. Alara Consultants cc, U.S.A.
- Hendriks P.H.G.M., Limburg J., de Meijer R.J., .Full-spectrum analysis of natural gamma-ray spectra. *J. Environmental Radioactivity* 53, 365 (2001).
- Idaho State University, (2005). Radioactivity in Nature. [www.isu.edu/NaturalRadioactivity.htm](http://www.isu.edu/NaturalRadioactivity.htm). (accessed 24/9/2005).
- International Atomic Energy Agency, (1989). Construction and Use of Calibration Facilities for Radiometric Field Equipment, Technical Reports Series No. 309, IAEA, Vienna.
- International Atomic Energy Agency, (1991). Airborne Gamma Ray Spectrometer Surveying, Technical Reports Series, No. 323, IAEA, Vienna.
- International Atomic Energy Agency, (2003). Guidelines for radioelement mapping using gamma ray spectrometry data, IAEA-TECDOC-1363, Vienna.

- Israeli Meteorological Services, (1994). <http://www.ims.gov.il/en1.htm>, (accessed 25/2/2006).
- Ivanovich, M., Harmon, R.S., (1982). Uranium Series Disequilibrium: Applications to Environmental Problems, Clarendon Press, Oxford.
- K. G. Vohra, eds. et. al., (1982). Natural Radiation Environment, (John Wiley & Sons), New York, U.S.A.
- Knoll G.F., .Radiation detection and measurement, third edition John Wiley & Sons, New York, (2000).
- Krane K. (1988). "Introductory Nuclear Physics", section 7.1, 7.3, 7.6. John Wiley & Sons, Inc. New York, 10158, U.S.A.
- Lahham A., Fulop M., (1997). A Mobile Whole-Body Counter for Accident and Occupational Monitoring of Internal Contamination. Radiation Protection Dosimetry, Vol. 71, No. 1, pp.41-45, Institute of Preventive and Clinical Medicine, Limbova 14, 83301 Bratislava, Slovak Republic.
- National Council on Radiation Protection and Measurements, (1987). "Exposure of the Population in the United States and Canada from Natural Background Radiation," NCRP Report No. 94, National Council on Radiation Protection and Measurements, Bethesda, MD, 61.
- Natural Resources Canada, (2004) , Airborne gamma-ray spectrometry, Canada, [http://gdcinfo.agg.nrcan.gc.ca/gdr/reports/agrs\\_e.html](http://gdcinfo.agg.nrcan.gc.ca/gdr/reports/agrs_e.html) (accessed 6/11/2005).
- NCRP, (1994). Exposure of the Population in the United States and Canada from Natural Background Radiation. NCRP Report No. 94. National Council on Radiation Protection and Measurements, Bethesda, Maryland.

- Nicholas A. Bertoldo (1998), Environmental Radiation Monitoring (LLNL Environmental Report, 12), Department of Energy, Ca, U.S.A.
- Norman E. and Rech G., (1996). A Schematic Diagram of the Radioactive Decay of  $^{137}\text{Cs}$ . [http://ie.lbl.gov/radioactivedecay/classes/bacs\\_frame2.htm](http://ie.lbl.gov/radioactivedecay/classes/bacs_frame2.htm) (accessed 14/6/2006).
- Otton J. (1994). Natural Radioactivity in the Environment, U.S. Geological Survey, Energy Resource Surveys Program, U.S.A. <http://energy.usgs.gov/factsheets/Radioactivity/radioact.html>, (accessed 28/9/2005).
- Peterson S. R., (1996). Experimental  $\gamma$  Ray Spectroscopy and Investigations of Environmental Radioactivity. Physics Department, the University of the South Sewanee, Published by Spectrum Techniques, Tennessee, U.S.A.
- Physics Atomic and Nuclear Physics Homework Help <http://www.brainmass.com/homeworkhelp/physics/atomicnuclearphysics/pg5> (accessed 23/2/2006).
- Taylor L., (1996). Radiation Past and Present, a Compendium. Sources of Radiation Exposure to the US Population. <http://www.fnrf.science.cmu.ac.th/theory/radiation/What%20You%20Need%20to%20Know%20about%20Radiation.html>, (accessed 14/6/2006).
- Tzortzis M., Tsertos H., (2002). Gamma ray measurements of naturally occurring radioactive samples from Cyprus characteristic geological rocks. Department of Physics, University of Cyprus, Nicosia, Cyprus.
- University of California, Santa Cruz, (2000). Radiation Safety Fundamental Workbook, Environmental Health and Safety, 4<sup>th</sup> Ed, California, U.S.A.
- Van Rooyen T.J., Lecture notes .The science of radiation protection., iThemba LABS, unpublished, (2002).

## دراسة النشاط الاشعاعي البيئي في منطقتي القدس وبيت لحم باستخدام مطيافية أشعة جاما الحقلية

### ملخص

تقدم هذه الدراسة تقديرا نوعيا وكميا للنشاط الاشعاعي البيئي في منطقتي القدس وبيت لحم. ولتحقيق ذلك استعملت تقنية مطيافية أشعة جاما الحقلية. يتكون نظام القياس من مكشاف اشعاع وميض (بلورة يوديد الصوديوم المطعم بعنصر الثاليوم) بحجم "3"×"3" انش متصل مع محلل طيف من نوع Inspect 2000 من شركة كانبيرا وكذلك مع جهاز كمبيوتر محمول. اما عملية قياس أطيف أشعة جاما فقد تمت بوضع المكشاف على ارتفاع متر واحد فوق سطح الارض. وقد أجريت القياسات في الحقل وكذلك في داخل البيوت في خمسة عشر موقعا. وتمت معايرة نظام القياس بطريقة تجريبية باستخدام مصادر لأشعة جاما ذات اشعاعية معروفة وكذلك بالطرق النظرية باستخدام النمذجة بواسطة طريقة Monte Carlo. ان اغلب العناصر المشعة التي تم التعرف عليها في التربة هي من العناصر المشعة الطبيعية التي تصدر اشعة جاما (نواتج انحلال اليورانيوم والثوريوم وكذلك نظير البوتاسيوم المشع  $^{40}\text{K}$ ) وقد تم اكتشاف مصدر مشع اصطناعي وحيد وهو عنصر السيزيوم  $^{137}\text{Cs}$  وذلك في موقعين في بلدة بيت ساحور وفي بلدة الدوحة بالقرب من بيت لحم. وأغلب التوقعات أن مصدر هذا العنصر هو حادثة مفاعل تشيرنوبيل التي حدثت في الاتحاد السوفيتي السابق عام 1986.

وتمت أيضا دراسة أثر الامطار في توهين أطيف أشعة جاما المنبعثة من التربة. وقد تبين ان الامطار تؤثر خاصة على الأجزاء من الطيف ذي الطاقات المنخفضة وبالأذات الاجزاء من طيف أشعة جاما التي تعود لنواتج انحلال عنصر اليورانيوم  $^{238}\text{U}$ . ويظهر أن توهين الفوتونات في تلك الأجزاء من

الطيف سببه انحباس غاز الرادون في التربة المشبعة بالماء بحيث يمنع هذا الماء انفلات غاز الرادون من التربة وبالتالي وصوله الى منطقة مكشاف الإشعاع. كذلك تم حساب معدل قراءات المكشاف داخل البيوت وخارجها ووجد أن هذا المعدل يتوافق مع نسبة معدل الجرعة الجامي خارج البيوت وداخلها.

لقد تم حساب إشعاعية كل من العناصر التالية  $^{208}\text{TI}$  و  $^{214}\text{Bi}$  ,  $^{40}\text{K}$  وكانت النتائج كالتالي:

( $177 \pm 26$  بكريل/كلغم) , ( $17 \pm 2.5$  بكريل/كلغم) و ( $14 \pm 2.1$  بكريل/كلغم) على التوالي. وكذلك اشتقت

تراكيز اليورانيوم والثوريوم وكانت ( $2 \pm 0.3$  جزء من مليون) لليورانيوم و ( $4 \pm 0.6$  جزء من مليون)

للتوريوم. أما حساسية نظام القياس فقد تم تحديدها عن طريق حساب النشاط الإشعاعي الأدنى الذي

يمكن قياسه لنظير البوتاسيوم المشع  $^{40}\text{K}$  وكانت القيمة 1 بكريل/كلغم.